

Sensitivity of Andean Glaciers to ice-flow parameters in the Parallel Ice Sheet Model

Ethan Lee¹, Jeremy C. Ely¹, Sarah L. Bradley¹, Tamsin L. Edwards², Bethan J. Davies³

¹ School of Geography and Planning, University of Sheffield, Sheffield, S3 7ND, UK

² Department of Geography, King's College London, London, WC2B 4BG, UK

³ School of Geography, Politics and Sociology, Newcastle University, Newcastle upon Tyne, NE1 7RU, UK

Correspondence to: Ethan Lee (ethan.lee@sheffield.ac.uk)

Abstract. Mountain glaciers are losing mass rapidly due to anthropogenic climate change. Projections of glacier evolution across the Andes under different warming scenarios have primarily been as part of global scale modelling frameworks, rather than dedicated, regionally optimised, simulations. These global-scale models use simplifications of ice flow physics that may be unsuitable for steep topography, such as that which occurs at mountain valley glaciers. More complex models are available, but with that complexity comes further sources of uncertainty. Here, we assess the sensitivity of the Parallel Ice Sheet Model to ice-flow parameters influencing the ice rheology and subglacial sliding characteristics. We find that the resistance of subglacial material has the most impact on modelled ice outputs (e.g., ice volume), followed by the exponent which relates basal shear stress to sliding, and the threshold velocity at which sliding occurs. The ice-flow rheology enhancement factors, the rate of subglacial water decay, and the maximum water thickness within a presumed subglacial drainage network, can either cause minor variations, or no effect at all, on ice outputs [in our model configuration](#). Our study informs what parameters can potentially be negated in future parameter ensemble tests and provides direction on where further investigation is needed.

Commented [EL1]: RC2 - Line 18

1 Introduction

Andean glaciers are a critical part of the region's water tower system (Immerzeel et al., 2020), particularly during droughts (Drenkhan et al., 2015) and in upland rural areas (Buytaert et al., 2017; Rabatel et al., 2013). However, they are losing mass rapidly (Dussaillant et al., 2019), placing stress on water resources, and contributing to sea level rise. Continued global warming, intensified by regional elevation-dependent warming (Byrne et al., 2024; Pepin et al., 2015), and changing precipitation regimes (Cai et al., 2020; Masiokas et al., 2020; Potter et al., 2023) heighten the need for accurate glacier projections to inform water management and sea level rise assessments.

Global-scale models of glaciers and ice caps (i.e., all land-based ice not stored in ice sheets) predict continued ice loss through to 2100 (Hock et al., 2019; Hugonnet et al., 2021; Rounce et al., 2020). While long-term sea level rise will be dominated by the Greenland and Antarctic Ice Sheets (Goelzer et al., 2020; Seroussi et al., 2024), glaciers and ice caps may contribute up to 0.35m of sea level rise by 2100 (Edwards et al., 2021; Hock et al., 2019; Marzeion et al., 2020). These global-scale experiments

32 are designed to capture the envelope of plausible sea level rise contributions from glaciers under different emission scenarios
33 (Fox-Kemper et al., 2023). However, global and regional scale projections of mountain glacier change are not only needed for
34 sea level rise, but also for management of changing water resources, mountain glacier hazards, resources for tourism and
35 recreation, and for ecological and biodiversity management.

36 Glacier models used in intercomparison efforts such as GlacierMIP (Hock et al., 2019; Marzeion et al., 2020; Rounce et al.,
37 2023) provide insight at global and regional scales (Zekollari et al., 2025). However, their use may be limited for planning
38 local resource management and mitigations due to: i) simplified ice-flow physics unsuited to steep topography (Egholm et al.,
39 2011); ii) reliance on downscaled global climate models (GCMs), which often poorly capture mountain climate (Núñez Mejía
40 et al., 2023); and iii) simplified mass balance schemes, often reduced to positive degree-day models (PDD; Bolibar et al.,
41 2022).

42 Here we attempt to address the first issue, by using a complex ice sheet model to assess uncertainties in the parameterisation
43 of glacier ice flow physics in areas of steep mountain topography. We use the Parallel Ice Sheet Model (PISM; Winkelmann
44 et al., 2011), a thermomechanically coupled shallow-ice/shallow-shelf model commonly applied to both ice sheets (Johnson
45 et al., 2023; Payne et al., 2021; Seroussi et al., 2024) and mountain glaciers (e.g., Candaş et al., 2020; Martin et al., 2022;
46 Žebre et al., 2021). PISM incorporates subglacial hydrology and basal sediment (till) deformation (Albrecht et al., 2020;
47 Winkelmann et al., 2011), but the added complexity increases the number of uncertain parameters. Perturbed parameter
48 ensembles are generally used to explore this type of uncertainty (e.g., Berdahl et al., 2021; Roe and Baker, 2014), however,
49 the number of simulations tends to increase with the number of parameters used, leading to significant computation for
50 computationally expensive models (Archer, 2024; Rougier, 2015). Therefore, a useful precursor to such efforts is a targeted
51 sensitivity analysis to identify which parameters meaningfully influence model outputs. This can aid in excluding parameters
52 from a full ensemble design that show low control over model output, saving computation resources and time.

53 The aim of this study is to assess the sensitivity of modelled Andean glaciers to ice-flow parameters within PISM. These
54 parameters include the ice-flow enhancement factors for the shallow-ice and shallow-shelf approximations, the subglacial
55 water decay rate, the maximum subglacial water thickness, the basal friction angle, the sliding exponent, and the velocity
56 threshold. We explore this parameter space through a suite of steady-state univariate and multivariate sensitivity experiments
57 across selected Andean glacier catchments. Model sensitivity is assessed by comparing percentage changes in simulated ice
58 volume and ice area, along with domain-mean ice thickness, and basal velocity relative to default parameter simulations in
59 each study catchment. We use Pearson correlation coefficients between parameter values and model outputs to assess
60 parameter influence over the model output. We first test grouped model components controlling ice deformation, subglacial
61 properties, and basal sliding, before conducting a more detailed analysis of the individual parameters that exert the strongest
62 influence on modelled outputs. We focus solely on parameters controlling internal ice deformation and glacier-bed interactions.

Commented [EL2]: RC2 - Line 53

Commented [EL3]: RC1 - Lines 54-55

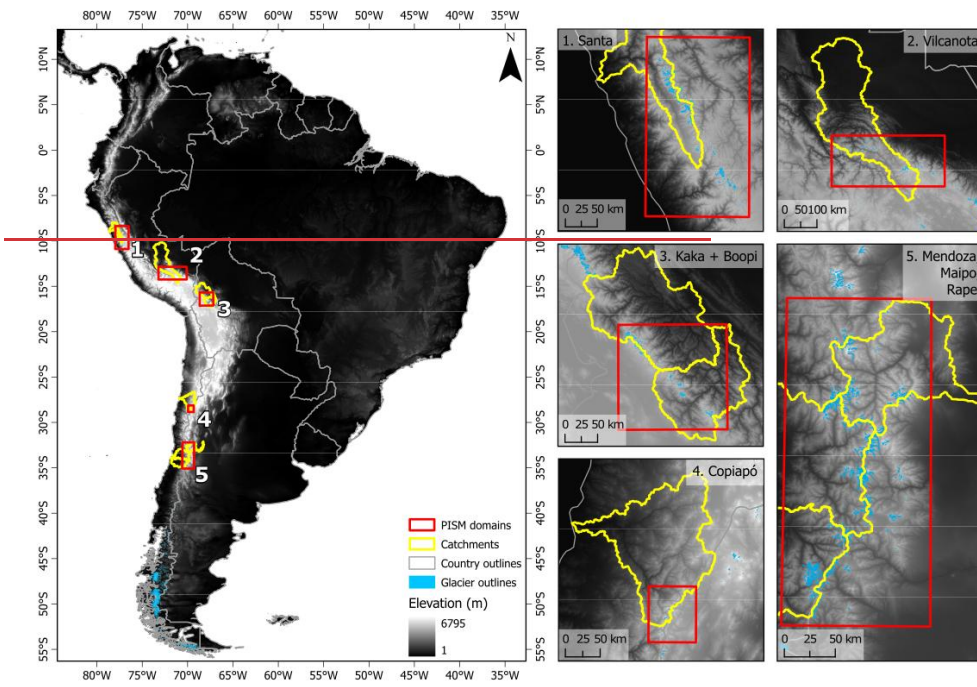
63

64 2 Study area

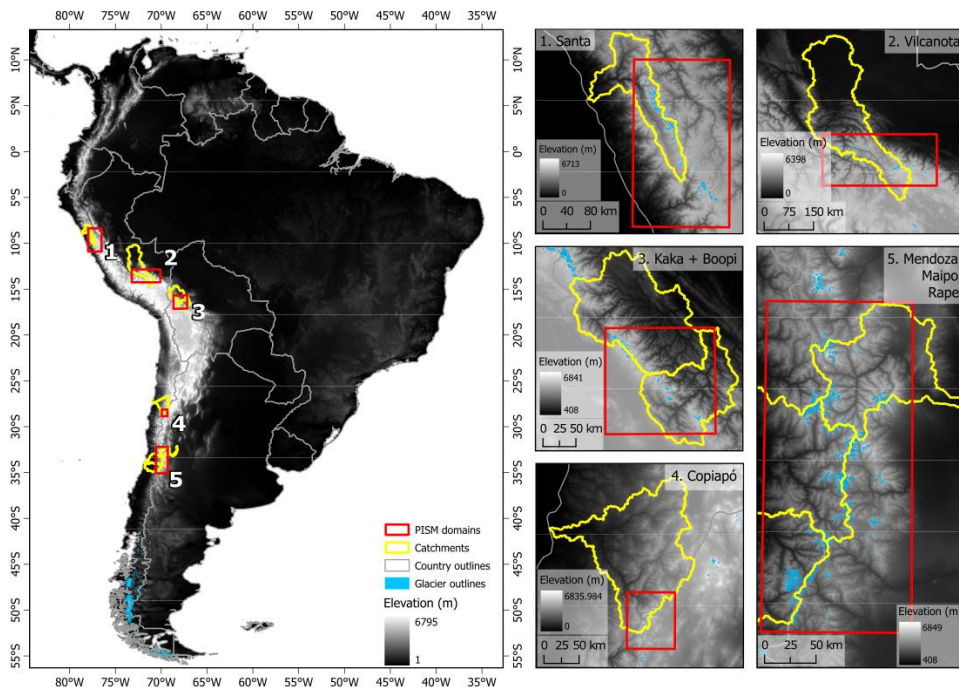
65 Mountain glaciers and ice caps in the Andes span 68° of latitude, from 12°N in Columbia, to 56°S in Chile and Argentina.
66 Projections over Andean glaciers show they are likely to become significantly smaller, or entirely lost, in the future due to
67 climatic warming (e.g., Zekollari et al., 2025). Rounce et al. (2023) estimates mass losses by 2100 for the Low Latitudes (RGI
68 16) of $69 \pm 25\%$ to $98 \pm 2\%$, and for the Southern Latitudes (RGI 17) $38 \pm 15\%$ to $68 \pm 20\%$ for the low and very high emission
69 scenarios RCP2.6 (mean projected global warming +1.6°C by 2100) and RCP8.5 (+4.3°C), respectively. Under the more recent
70 SSP scenarios, Rounce et al., (2023) projected slightly higher losses: from $76 \pm 18\%$ to $99 \pm 3\%$ in the Low Latitudes, and
71 from $49 \pm 19\%$ to $74 \pm 22\%$ in the Southern Andes, under SSP1-2.6 (+1.8°C) and SSP5-8.5 (+4.4°C), respectively. More
72 recently, Zekollari et al. (2025) ~~detailing-assessed~~ the committed loss of glaciers after ~~reaching equilibrium equilibrating~~ with
73 global warming estimates of +1.5°C and +4.0°C. ~~They estimated that~~ the Southern Andes would lose a mean of 45% and 79%
74 of their mass ~~under these warming levels~~, and the Low Latitudes a mean of 46% and 96% of their mass respectively. Regionally
75 specific in Peru, Drenkhan et al. (2015) projects area losses between 40.7% and 44.9% by 2060 under RCP2.6, and between
76 41.4% and 92.7% by 2100 under RCP8.5.

77 The five PISM model domains used in this study encompass the mountain glaciers in the 1) Santa, 2) Vilcanota, 3) Kaka and
78 Boopi, 4) Copiapó and 5) Mendoza, Maipo, and Rapel hydrological catchments (Fig. 1). The glaciers in these hydrological
79 catchments are particularly important for their role as meltwater sources for downstream populations (Masiokas et al., 2020;
80 Vuille et al., 2008). The chosen domains cover three different climatological zones: domains 1, 2, and 3 are within the tropical
81 Andes, with a diurnal temperature variation that outweighs the annual temperature variation. This leads to glaciers ~~persisting~~
82 ~~at high elevations~~, being sensitive to changes ~~in in-~~precipitation, that impact the presence and distribution of snowfall across
83 the glacier surface (Hardy et al., 1998; Kaser, 1999). Domain 4 lies within the desert Andes, with high snowline altitudes. This
84 arid climate has short snowfall events that cause glaciers to lose mass primarily through sublimation (Fyffe et al., 2021;
85 Masiokas et al., 2016). Lastly, domain 5 comprises three adjacent mountain hydrological catchments within the wet Andes
86 that are sensitive to temperature changes, due to receiving substantial snowfall during the winter months (Masiokas et al.,
87 2016), while the presence of glacial lakes enhances mass loss through calving and proglacial lake-driven melting (Wilson et
88 al., 2018).

Commented [EL4]: RC1 - Lines 65-67



89



91 **Figure 1: Chosen hydrological catchments and the five PISM domains across the South American Andean Mountains used in this**
 92 **sensitivity analysis. Red outlines show the model domains, focused on glaciated areas within each hydrological catchment.**
 93 **Hydrological catchment boundaries are from HydroSHEDS (Lehner et al., 2008). Elevation for each domain taken from the sub**
 94 **figure scene. The domain statistics are found in Table 2.**

95 The Andes have been the focus of numerous studies examining glacier extent changes in response to both centennial (e.g.,
 96 Carrivick et al., 2024; Emmer et al., 2021) and decadal scales (e.g., Dussaillant et al., 2019; Taylor et al., 2022). Global-scale
 97 studies using simplified two-dimensional flowline models (e.g., OGGM; Maussion et al., 2019) have modelled individual
 98 Andean glaciers as part of broader global modelling frameworks, which apply a uniform modelling frameworks-approach
 99 across diverse climatic and topographic regimes. Although these global frameworks can assimilate regional climate data, they
 100 do not specifically optimise for Andean glacier dynamics and are unable to account for highly heterogenous climatic regimes
 101 such as those of Andean glaciers. However, regional-scale glacier modelling specific to the Andes remains limited. Most
 102 physically based modelling efforts have been concentrated on the Patagonian Icefields, a setting distinct from the rest of the
 103 Andes, while other studies are primarily focused on modelling from the Last Glacial Maximum to present (e.g., Cuzzzone
 104 et al., 2024; Martin et al., 2022; Wolff et al., 2023; Yan et al., 2022). To date, only one study has focused in detail on modelling

105 Andean Mountain glaciers outside Patagonia, assessing their response to climate extremes, however, this study is restricted to
 106 just two glaciers (Richardson et al., 2024). Consequently, parameter choices and process understanding for physically based
 107 modelling of Andean glaciers remain poorly constrained.

108

109 3 Materials and methods

110 3.1 Parallel Ice Sheet Model

111 Here, we used the Parallel Ice Sheet Model (PISM v2.1) (Winkelmann et al., 2011) to conduct our numerical modelling. PISM
 112 is an open-source, three-dimensional, thermomechanically coupled, hybrid shallow ice, shallow shelf, approximation ice sheet
 113 numerical model. The parameter combinations of PISM can be calibrated to represent localised climate and glaciological
 114 conditions when sufficient observational constraints (e.g., mass balance data, surface velocity, past glacier extents) are known.
 115 Otherwise, default parameter values, which have primarily been tuned for the Greenland Ice Sheet, are set automatically if not
 116 specified. Key parameters we have chosen to change here are mentioned throughout the following sections and in Table 1,
 117 together with their PISM default values and the minimum and maximum values used in our sensitivity experiments. These
 118 ranges were informed by values used in previous modelling studies, as discussed below, but were deliberately extended beyond
 119 commonly applied ranges to test the response of model outputs under a wide parameter space.

120 Table 1: Chosen glaciological model parameters for sensitivity analysis within PISM. Letters on the leftmost edge of the table
 121 correspond to the component letter within PISM that the chosen parameters cover, the minimum and maximum values chosen are
 122 explained within the main text. Default values are those set within the PISM code, which is also explained in the main text. All
 123 other parameters not mentioned within this table are left at their default values, which can be found in PISM's Configuration
 124 Parameters online manual (<https://www.pism.io/docs/manual/parameters/index.html>).

	Parameter	Default	Min	Max		Description
E	E_{SIA} / E_{SSA}	1	0.2	20	-	Enhancement factor for SIA and SSA: E_{SIA} and E_{SSA} are multipliers on the ice softness, E_{SSA} controls how easily the ice deforms.
T	C	1	0.1	12	mm/a	Subglacial water decay rate: determines the amount of water discharge from a hypothetical layer of water beneath the glacier, conceptually this is presumed to be stored in sediment, but could also apply to subglacial cavities.
	W_{till}^{max}	2	0.1	10	m	Maximum subglacial water thickness: the amount of effective water thickness within the subglacial environment; all water above this is not retained.
	ϕ	30	5	45	°	Subglacial bed strength: a parameter in the Mohr-Coulomb criterion for yield stress, which is a shear strength parameter related to the geology of the bed.

Commented [EL5]: RC1 - Line 123-124

Commented [EL6]: RC1 - Table 1

Commented [EL7]: RC2 - Table 1 Line 109

S	q	0.25	0.05	0.95	-	Sliding exponent: controls the relationship between basal shear stress and sliding velocity within the Zoet and Iverson (2020) slip law.
	$u\mathcal{H}_{threshold}$	100	20	200	m/a	Velocity threshold: the velocity above which sliding occurs at the base of the ice.

125

126 3.1.1 Enhancement Factors (E Component)

127 We used PISM’s hybrid shallow ice shallow shelf approximation (hybrid SIA+SSA). This is the combination of the shallow-
 128 ice (SIA; Hutter, 1983; Mangeney and Califano, 1998) and shallow-shelf approximations (SSA; Bueler and Brown, 2009;
 129 Weis et al., 1999), enabling PISM to represent both the vertical deformation and longitudinal stretching of the ice, along with
 130 basal sliding. This hybrid SIA+SSA has been applied in other [mountain](#) valley-based glacial systems (e.g., Candaş et al., 2020;
 131 Gollledge et al., 2012; Martin et al., 2022; Seguinot et al., 2018).

132 The stress balance, and the resulting rate of ice deformation ($\dot{\epsilon}$), is described by the Glen-Paterson-Budd-Lilboutry-Duval flow
 133 law (Lilboutry and Duval, 1985). This is the default enthalpy-based flow law within PISM, shown in Eq. 1,

$$\dot{\epsilon}_{ij} = EA(T, \omega)\tau^{n-1}\tau_{i,j}, \quad (1)$$

134 where E is the enhancement factor, A is the ice softness, T is the ice temperature, ω is the liquid water fraction, τ is the stress
 135 imposed on the ice, and n is the Glen’s flow law exponent. E is implemented for both the SIA and SSA, acting as a multiplier
 136 on the ice softness inferred from A . Therefore, higher values are likely to represent softer ice that deforms more readily, while
 137 lower values of E represent stiffer ice.

138 For the sensitivity tests, we changed the parameterisation of E for both the SIA and SSA. Many studies have varied E_{SIA} with
 139 values between 1 and 6 (Candaş et al., 2020; Ely et al., 2024; Johnson et al., 2023; Zinck and Grinsted, 2022), and E_{SSA} between
 140 0 and 1.5 (Martin et al., 2022; Seguinot et al., 2018; Yan et al., 2023). We varied both E_{SIA} and E_{SSA} at the same time between
 141 0.2 and 20 (see Table 1). This wider range was used due to previous observations of E for SIA within lab studies have found
 142 values between 1.3 and 10.2 (Treverrow et al., 2012), and up to 120 in field studies over the Urymqi Glacier No. 1 in China
 143 (Echelmeyer and Zhongxing, 1987). While no observations of E for the SSA are detailed, modelling studies (as shown above)
 144 have used narrower values. By applying an extended range to both E for SIA and SSA, we aim to test whether strongly reduced
 145 or enhanced deformation could substantially affect modelled output ice volume, thickness, and velocity, and therefore whether
 146 these parameters should be prioritised in future parameter ensembles.

147

148 3.1.2 Subglacial properties (T Component)

Commented [EL8]: RC2 - Line 109

Commented [EL9]: RC2 - Line 121

149 In PISM, the subglacial hydrology and sliding scheme was originally developed for ice-sheet contexts and conceptualises the
150 bed as a deformable layer, to represent subglacial ‘till’ or sediment, that can store water and influence basal resistance (Albrecht
151 et al., 2020). We therefore refer to these parameters collectively as the “T component”, where “T” denotes till-related subglacial
152 properties. The extent to which this subglacial sediment is under ice sheets is unknown, which is also the case for Andean
153 glaciers (Cuffey and Paterson, 2010); although/Although, thick layers of sediment are present-common in mountain glacier
154 forefields due to repeated glacier advance and retreat phases, and meltwater reworking (e.g., Carrivick and Heckmann., 2017;
155 Lee et al., 2022). However, the formulation for glacier sliding and hydrology does not require, and should not be interpreted
156 as, sediment to be present everywhere beneath the glacier. The effective pressure and sliding behaviour can equally represent
157 hard-bedded conditions, where subglacial water storage may occur within bedrock cavities rather than within sediments
158 (Cuffey and Paterson, 2010; Zoet and Iverson, 2020). ~~To note~~Therefore, while we use the term ‘till’ throughout this study for
159 consistency with PISM terminology and previous studies, it should not be interpreted as implying continuous sediment cover
160 beneath Andean glaciers.

Commented [EL10]: RC1 - Line 126

161 The yield stress of the basal material (τ_c) in PISM is calculated using the Mohr-Coulomb criterion, which incorporates the till
162 friction angle ~~till friction angle~~ (ϕ), a parameter influenced by the underlying bed geology (Albrecht et al., 2020; Cuffey and
163 Paterson, 2010). This relationship is partly governed by PISM’s subglacial hydrology model. The Mohr-Coulomb criterion
164 used to compute yield stress is given in Eq. 2,

Commented [EL11]: RC1 - Line 128-133

$$\tau_c = c_0 + (\tan\phi)N_{till} \quad (2)$$

Commented [EL12]: RC2 - Line 135

165
166 Where c_0 is the till cohesion that uses a default value of 0 (Schoof, 2006), and N_{till} is the effective pressure at the base of the
167 ice within the till layer. For every domain we applied a spatially uniform ϕ . Previously used values of ϕ have generally been
168 within ranges of values 5-45°, derived from lab-based experiments of different till types (Cuffey and Paterson, 2010; Koloski
169 et al., 1989). Lower values of ϕ represent a weak, slippery bed that promotes basal sliding due to a low yield threshold, while
170 higher values represent a strong, rigid bed that increases basal friction and makes sliding harder to occur. The default value in
171 PISM is 30°, while in the sensitivity tests, we varied ϕ between 5° and 45° (see Table 1).

Commented [EL13]: RC2 - Specific Comments

172 Within Equation 2, N_{till} is determined in part by the hydrology beneath the ice. The hydrological model used here is a non-
173 conserving model (Tulaczyk et al., 2000). This does not allow the conservation of any water above an assigned till water
174 thickness (W_{till}^{max}). This is where W_{till} is constrained between 0 and the prescribed W_{till}^{max} value. Any water exceeding this is
175 removed from the till water layer and is not retained. The thickness of the water layer stored within the till is determined by
176 Eq. 3,

Commented [EL14]: RC2 - Line 149

$$\frac{\partial W_{till}}{\partial t} = \frac{m}{\rho_w} - C \quad (3)$$

Where m is the basal melt rate, ρ_w is the density of fresh water (1000 kg m³), and C is the till water decay rate that denotes how fast water is evacuated from the till water (Albrecht et al., 2020; Flowers, 2015). At all times within the model, $0 \leq W_{till} \leq W_{till}^{max}$ must be satisfied, with any water above W_{till}^{max} being removed.

C and W_{till}^{max} are tested in our sensitivity analysis through the T Component. To our knowledge, no previous PISM studies have varied C over mountain glaciers, although PISM ice sheet studies have used values between 1 to 10 mm yr⁻¹ (Albrecht et al. (2020)). Higher values of C drain the till faster, analogous to efficient drainage systems, that is likely to cause less sliding overall, while lower values of C represent a more inefficient drainage, leading to more water within the till and likely allowing more sliding to occur. Here we vary C between 0.1 and 12 mm/a.

For W_{till}^{max} previous PISM mountain glacier studies have used values between 1 to 5 m (Candaş et al., 2020; Žebre et al., 2021). High values of W_{till}^{max} allow more water to be retained within the till at the base of the ice, increasing water pressure therefore decreasing the effective pressure (N_{till}) allowing more sliding to occur. The till water decay rate is varied between 0.1 and 12 mm/a, while the W_{till}^{max} maximum till water thickness is varied between 0.1 and 10 m (see Table 1). These ranges either extend beyond previously used values for mountain glacier modelling studies, or applied ranges that have been used over ice sheet scales, aiming to assess whether either parameter has a substantial influence on modelled output of ice volume, thickness, or basal velocity.

Commented [EL15]: RC2 - Line 151

3.1.3 Basal sliding (S Component)

In PISM, basal sliding is represented by relating the basal shear stress (τ_b) to both the ice velocity (u) and effective pressure (N). A velocity threshold ($u_{threshold}$) marks when τ_b equals the yield stress (τ_c), and therefore when sliding occurs (Cuffey and Paterson, 2010). By default, within PISM we used the Zoet and Iverson (2020) slip law, which introduces a regularisation term that enables a smooth transition between the viscous-style Weertman sliding (Weertman, 1957), and the Coulomb-plastic behaviours (Aschwanden et al., 2013), without needing prior knowledge of bed type. The Zoet and Iverson (2020) slip law is expressed in PISM by Eq. 4,

$$\tau_b = -\tau_c \frac{u}{(|u| + u_{threshold})^q |u|^{1-q}}, \quad (4)$$

Zoet and Iverson (2020) in their equation parameterise $q = 1/m$ where $m = 5$, whereas PISM's default value of q is 0.25 (or where $m = 4$). While the Zoet and Iverson (2020) slip law is relatively new in PISM, being introduced in v2.0, few PISM

203 studies have utilised it. Those modelling efforts that have used the Zoet and Iverson (2020) slip law, (e.g., the Community Ice
204 Sheet Model or CIESM; Lipscomb et al., 2019), have varied it between narrow ranges. These have been at 0.2 (Khan et al.,
205 2022; Moreno-Parada et al., 2023), 0.23 (Maier et al., 2022), or 0.33 (van den Akker et al., 2025; Hoffman et al., 2022; Joughin
206 et al., 2024). Within our sensitivity analysis, q and $u_{threshold}$ were tested through the S component.

207 We varied q from 0.05 to 0.95 to maximise the coverage of potential parametrisations of q to the extremes. Due to the use of
208 the Zoet and Iverson (2020) slip law in this study, increasing the value of q can lead to decreased resistance where there are low
209 to moderate basal velocities, or where it is near the onset of sliding, increasing velocities in those areas. Where there are the
210 fastest velocities (i.e., ice flowing into valleys), there is likely to be minimal effect on their velocities due to basal shear stress
211 already being at, or near, to the yield stress.

Commented [EL16]: RC2 - Specific comments

212 We also varied $u_{threshold}$, a parameter that has seen ~~some~~ variation for sensitivity or optimisation within a limited number of
213 studies to our knowledge. ~~in other modelling studies (Bevan et al., (2023; Martin et al., 2022; Seguinot et al., 2014, 2018),~~
214 ~~applied the BISICLES ice sheet model to the Amundsen Sea Embayment in West Antarctica, used values between 20 to 600~~
215 ~~m/a. Due to the $u_{threshold}$ only being varied over ice sheet settings, we varied the $u_{threshold}$ between 20 and 200 m/a (see~~
216 ~~Table 1). The maximum value we use takes into account the mountain glacier setting we are studying: s mountain glaciers are~~
217 ~~unlikely to reach the high velocities that are achieved by ice streams (>200 m a⁻¹); It is anticipated that higher parameter values~~
218 ~~for $u_{threshold}$ would lead to sliding occurring over less of the glacier, but higher maximum basal velocities. Higher thresholds~~
219 ~~will delay the transition to Coulomb-limited sliding, but once the threshold is exceeded, higher sliding velocities will occur.~~
220 ~~Conversely, decreases in the $u_{threshold}$ are likely to lead to larger portions of the glacier experiencing sliding, but lower~~
221 ~~maximum velocities.~~

Commented [EL17]: RC2 - Specific Comments

Commented [EL18]: RC2 - Specific comments

223 3.1.4 Surface mass balance

224 We used PISM's default positive degree day (PDD) temperature-index scheme (Calov and Greve, 2005) to generate ice within
225 the domains. This required monthly mean air temperature and yearly precipitation (see Sect. 3.3).

226 Within the PDD scheme, there is stochastic 'white noise' to simulate additional undetermined daily variability, as well as a
227 daily temperature standard deviation that is set by default at 5°C (Winkelmann et al., 2011). We acknowledge that the treatment
228 of sub-monthly temperature variability within the PDD model can influence simulated melt and is therefore another source of
229 uncertainty within the model (Seguinot, 2013).

230 ~~These can cause minor fluctuations in the climate, and thereby in the ice extent even under steady state conditions. We forced~~
231 ~~the model with a constant present-day climate (see Sect. 3.3), to allow glacial ice to reach steady state with its surrounding~~
232 ~~climate. As this study is focused on purely parameters that influence ice flow, Pparameters that affect the PDD model~~

component of PISM, such as degree day factors, were kept at their default values and not varied within this study, due to these values being unknown and this study only being concerned with the internal ice model parameters. Any minor fluctuations in steady-state ice extent associated with the PDD scheme are consistent across the ensemble and do not affect the relative comparison between ice-flow parameter perturbations.

Commented [EL19]: RC2 - Line 175

3.2 Model setup and parameter sensitivity analysis

The five model domains simulated by PISM are shown in Fig. 1. Each domain had a 100 m horizontal grid resolution (dimensions in Table 2), with 50 vertical ice layers spaced quadratically, and 10 bedrock layers. These vertical layers were chosen to resolve near-basal ice interactions where thermal and sliding-related processes are important, further this horizontal resolution was chosen as it can resolve the topography and flow characteristics while maintaining feasible wall-clock run times (e.g., Lee, 2024). No separate sensitivity test was performed for vertical and horizontal resolution set up, however this was kept the same for all model runs. All domains were initialised without prescribed ice thicknesses, allowing mountain glaciers to grow from no ice conditions, and run to steady state (~1,500 model years) under constant climate forcing (see Section 3.2).

Commented [EL20]: RC1 - Lines 184-185

Commented [EL21]: RC1 - Line 186

Table 2: PISM study domains, detailed with their grid x, y, sizes at 100 m resolution, and the domain area, along with the RGIv7 ice area of each domain, and the elevations from the ALOS DEM, for each domain all at 100 m resolution. The location of each domain, and the hydrological catchments they partially cover, are shown in Fig. 1.

Commented [EL22]: RC2 - Specific comments

Domain	x	y	Area (km ²)		Elevation (m)		
			Domain Area (km ²)	Ice Area (km ²)	Min	Max	Mean
1) Santa, Peru	1600	2800	44,800	607	0	6731	3337
2) Vilcanota, Peru	3400	1600	54,400	515	241	6289	3273
3) Kaka and Boopi, Bolivia	1600	1600	25,600	240	481	6401	3187
4) Copiapó, Chile	600	800	4,800	35	1437	5845	4108
5) Mendoza, Maipo, and Rapel, Chile	1200	3600	43,200	1,303	601	6927	3085

Our sensitivity analysis focused on internal ice-flow parameters. These parameters define the physical properties and processes governing ice behaviour, such as the shallow ice, and shallow shelf approximation (SIA/SSA) flow enhancement factor, basal sliding, and subglacial mechanics. We targeted parameters that: (i) have shown substantial influence on glacier modelling in previous studies; (ii) are commonly tested in sensitivity analyses; and (iii) remain poorly constrained by observations or past modelling.

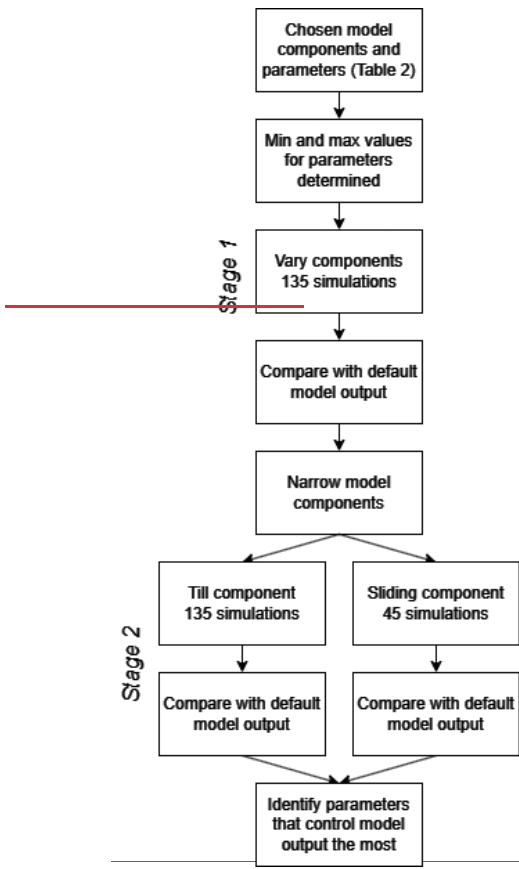
The analysis followed a two-stage approach (Fig. 2) to enable efficient identification of components that exert the greatest control over model outputs. This coarse screening (Stage 1) allowed subsequent parameter-specific tests (stage 2) to focus only

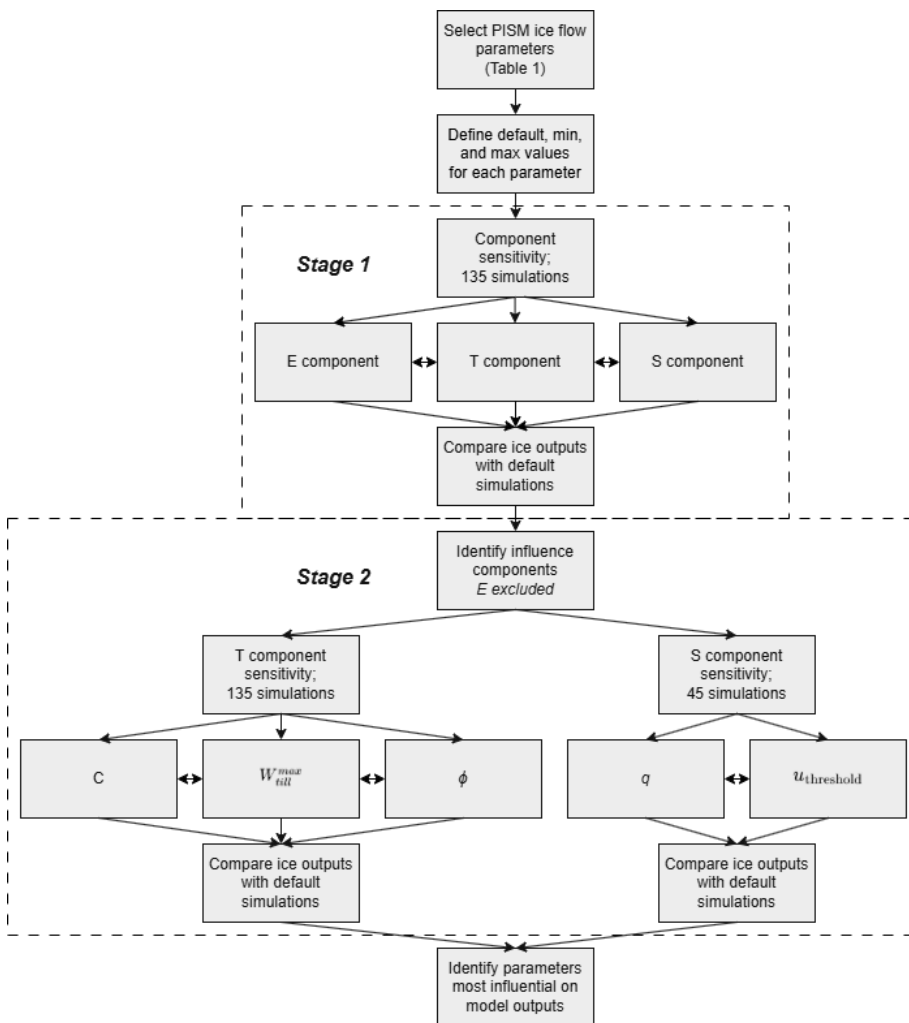
258 on the most sensitive components governing ice flow. This aim of this is to reduce the dimensionality of the analysis and the
259 computational cost of future ensemble experiments. This two-stage approach can be used by other sensitivity studies to
260 facilitate more efficient sampling of key aspects of the model in question that causes the most effect on chosen outputs.

261 In stage 1 (135 model simulations: 27 per domain), we group individual parameters into components impacting three key ice-
262 flow processes: enhancement factors (E), basal sliding (S), and subglacial properties (T). The parameter values applied span
263 beyond both those commonly used and extended ranges to capture a broad spectrum of glacier responses, see Section 3.1 for
264 details. Each component was perturbed between its chosen minimum, maximum, and default values (Table 1), first individually
265 (with all other components fixed at default values) and then simultaneously, to generate the ensemble design for each domain
266 (see SI Table 1 for an example). Components that showed negligible influence on outputs were discarded from further analysis.

Commented [EL23]: RC1 - Lines 200-205

Commented [EL24]: RC1 - Lines 200-205





268
269 **Figure 2: Workflow of the two-stage sensitivity experiment design used here. Stage 1 tests the influence of the chosen model**
270 **components: the enhancement factors (E), till-related parameters (T), and sliding parameters (S). These use the default, minimum,**
271 **and maximum parameter values from Table 1. Components with limited influence are excluded from Stage 2. Stage 2 then tests**
272 **individual parameters within the retained T and S components to identify which parameters exert the most influence on modelled**

273 ice volume, thickness, and basal velocity. Simulation numbers are shown for the full five-domain ensemble. These were varied both
274 individually and all together. Flow diagram of sensitivity experiment design detailing the staged approach.

275 Stage 2 (180 model simulations: 36 per domain) comprised a detailed within-component analysis of only those components
276 identified in Stage 1 as influential. Here, every individual parameter was perturbed one-at-time across their defined value
277 ranges (min, max, default; Table 1), followed by simultaneous perturbation of all parameters within that component, rather
278 than grouping them by component as in Stage 1. Parameter in each figure and table corresponds to a shortened name presented
279 here; enhancement factor (E), till water decay rate (C), maximum till water thicknesses (T_m or W_{till}^{max}), till friction angle (Phi
280 or ϕ), sliding exponent (q), velocity threshold (Uth or $uU_{threshold}$).

281 Model outputs, of ice volume, ice thickness, and basal velocity, were compared against the baseline simulation using the
282 default values for all parameters. To quantify influence, results were averaged over the domain and Pearson correlation
283 coefficients were calculated between these and the parameter values, along with p-values to assess statistical significance of
284 their effect. This approach provided both a ranking of parameter sensitivity and an assessment of the robustness of their effects.

285 3.3 Boundary conditions data

287 Topography is a key initial condition within PISM. We used the ALOS 30 m DEM (Tadono et al., 2014), due to its accuracy
288 over complex mountainous terrain (Talchabhadel et al., 2021), resampled to 100 m using a bilinear interpolation. Basal
289 topography was derived by subtracting present-day ice thicknesses of Millan et al. (2022) from the ALOS DEM.

290 Geothermal heat flux is required to define and apply the temperature of the bed to the base of the ice. We used Geothermal heat
291 flux was prescribed from Davies (2013) which uses the relationship between basal heat flux to geology on a 2°×2° global grid.

292 Due to the lack of regional specific geothermal heat flux estimates within our study areas and the coarse nature of the dataset,
293 for each domain we assigned a single value based on the value from the grid cell containing the most glacial ice.

294 Climate input is required for the PISM PDD scheme. For our present-day climate, we used the WorldClim 2.1 data (Fick and
295 Hijmans, 2017). WorldClim 2.1 is a gridded climate data for the years 1970-2000 collected from weather stations here we use
296 the average air temperature (K) and average total annual precipitation (mm yr⁻¹), resampled from a grid resolution of ~900 m
297 to 100 m bilinearly. Due to air temperatures from WorldClim being based on the 30 arc second SRTM DEM, it underestimates
298 temperatures across mountain peaks. To remedy this, we applied the global average a-lapse-rate correction of 6.5°C/km across
299 the entire temperature field, based on elevation differences between the WorldClim SRTM and resampled ALOS DEMs.

300 Erroneous adjustments due to DEM artefacts were removed and interpolated across linearly. We acknowledge that the chosen
301 lapse rate correction of the temperature field can itself present some uncertainty. Ultimately, the purpose of the climate forcing
302 in this study is not to reproduce the exact present-day size and shape of each glacier, but to generate steady-state ice extent
303 within each domain from which we can determine the sensitivity to ice-flow parameters. we are not concerned about the size

Commented [EL25]: RC1 - Lines 224-225

Commented [EL26]: RC2 - Line 232

Commented [EL27]: RC2 - Line 234

Commented [JE28R27]: good

304 and shape of the glaciers produced. The role of the climate forcing is simply to produce some ice from which we can understand
305 model sensitivity from.

307 4 Results and Discussion

308 Here, we outline results from the Stage 1 component sensitivity experiments for simulated volume change, then for the
309 subsequent Stage 2 parameter sensitivity experiments, for all domains. Aggregated domain results are shown here, with
310 individual model simulation outputs (area, volume, and percentage changes for each domain) available in the Supplementary
311 Information (SI): component sensitivity (SI Tables 1–5), subglacial parameter sensitivity (SI Tables 6–10), and sliding
312 parameter sensitivity (SI Tables 11–15). Final time-slice outputs of ice thickness and ice velocities, along with their differences
313 with the default model simulation for their respective regions, are shown in SI Figures 1–40. Key examples of these are shown
314 throughout which are also shown in the SI for ease of comparison. As the ice area was largely unaffected by parameter
315 changes, they are not shown within the sensitivity bar graphs for transparency, but focus the main
316 discussion on ice-volume change only. Volume outputs are discussed in any detail, though area is shown in some figures for
317 comparison.

Commented [EL29]: RC1 - Lines 244-245

319 4.1 Stage 1 – Model component sensitivity analysis

320 Stage 1 is used to determine which model component influences the ice metrics the most, to guide the more detailed Stage 2
321 sensitivity analysis (Table 3; Fig. 3). We describe results for each component in turn here.

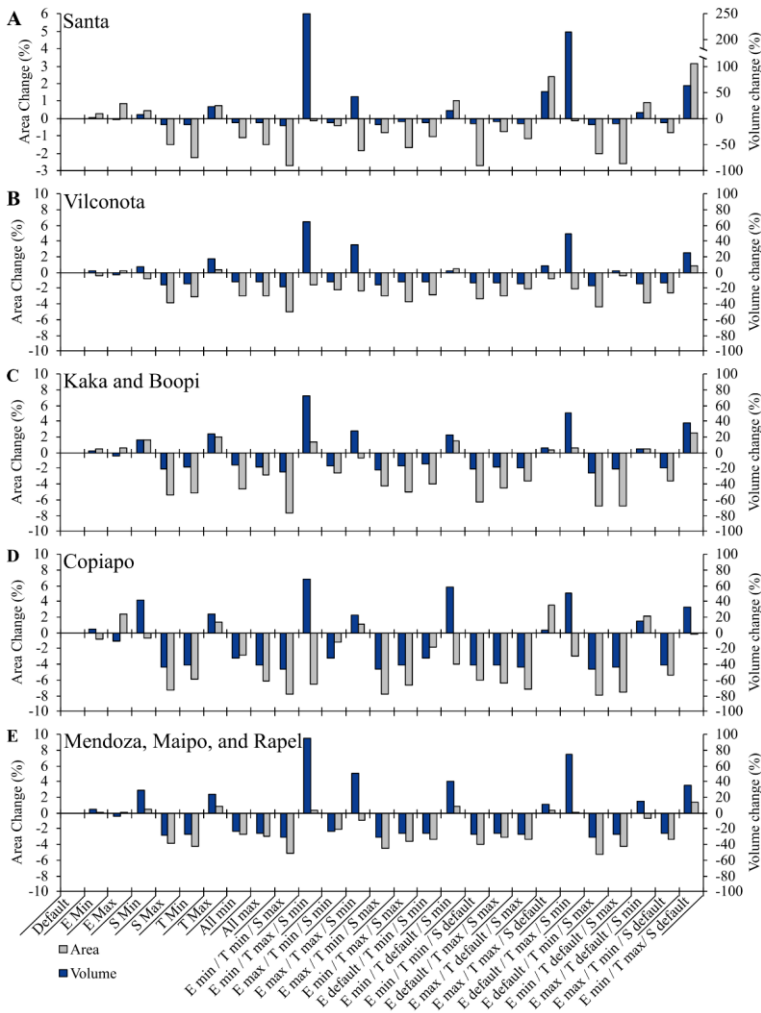
322 When varying E component parameters (E_{SIA} and E_{SSA}) were varied between their minimum and maximum values (Table 1)
323 resulted in ice volume changes of +5.4% to -9.9% from their defaults across all domains. These changes are reflected primarily
324 in ice thickness (Fig. 4), with maximum E values producing thinner ice (mean: -5.4%) and increased basal velocities (mean:
325 +4.8%), though the Vilcanota (#2) domain showed a velocity decrease of -11.9%. Minimum E values led to thicker ice (mean:
326 +3.2%) and reduced velocities (mean: -9.1%). Pearson correlations between E and ice volume were weak and statistically
327 insignificant across all domains ($p > 0.53$; Table 4).

Commented [EL30]: RC1 - Line 251

328 Table 3: Initial sensitivity analysis outputs detailing the default model simulation volume, and the maximum absolute percentage
329 changes for volume for each domain across the ensemble when components were varied between their maximum and minimum
330 values.

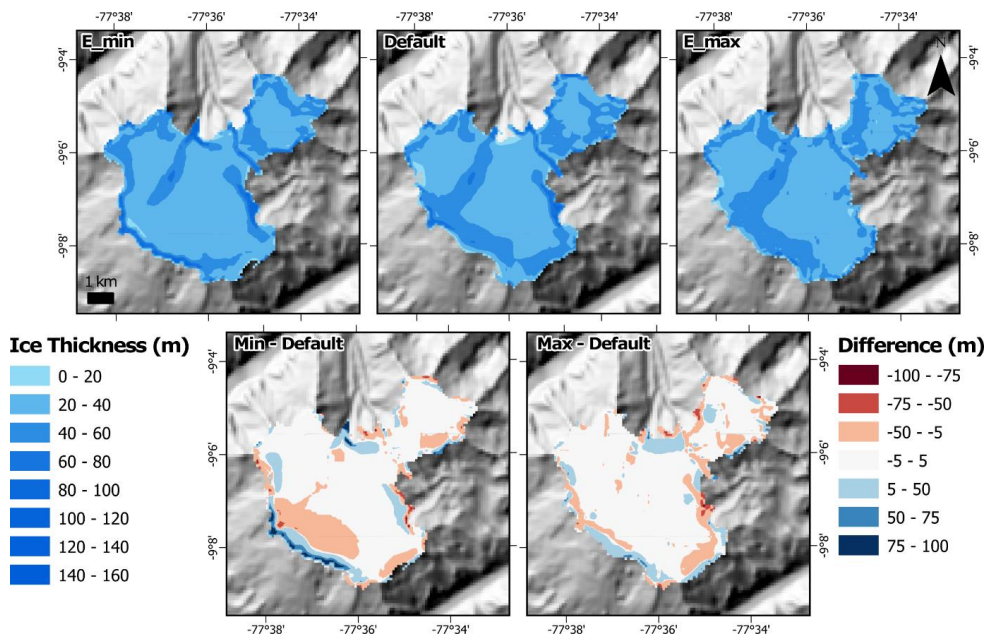
Domain	Volume (km ³)			Max abs change (%)
	Default	Max	Min	
Santa	10.1	35.2	8.8	247.2

Vilcanota	3.1	5.1	2.5	64.1
Kaka & Boopi	2.2	3.8	1.6	71.8
Copiapó	1.1	1.9	0.6	68.5
Mendoza, Maipo & Rapel	17.6	34.4	12.1	95.2



332

333 **Figure 3: Initial sensitivity analysis detailing the area (grey) and volume (blue) absolute change percent due to changing all model**
 334 **component parameters together, for each of the five model domains. Blue and grey lines denote the default volume and area**
 335 **respectively for comparison. Component parameters are: E = enhancement factors, T = subglacial component, S = sliding**
 336 **component. See Fig. 1 for model domain locations. Note the break in y-axis for ice volume in A) detailing the significant increase in**
 337 **volume, above +200%.**



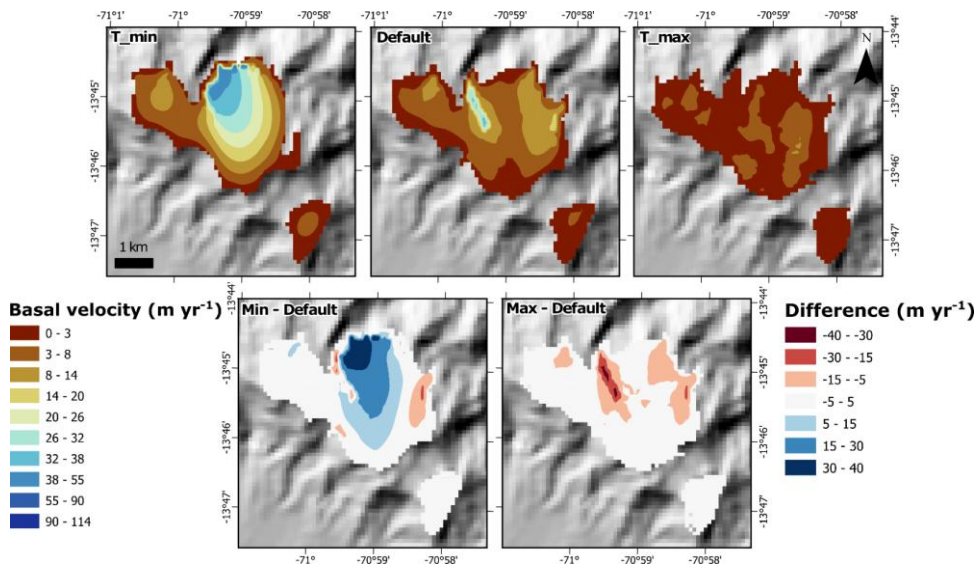
338
 339 **Figure 4: Example of the influence of the enhancement factors on simulated ice thickness in the Santa (#1) domain (Huascarán Ice**
 340 **Cap). Additional examples are provided in the Supplementary Information. Ice peripheral differences in ice thickness are likely to**
 341 **arise from internal variability in the PDD model as mentioned previously in Sect. 3.3, despite a temperature standard deviation of**
 342 **5°C. Parameter values for ‘max’ and ‘min’ are listed in Table 1.**

343 Similar results - i.e., non-significant variations in modelled outputs - were reported using PISM in other mountain glacier
 344 settings (Candaş et al., 2020; Martin et al., 2022) and for ice caps (Schmidt et al., 2020). More substantial effects from the
 345 enhancement factors that impact ice rheology, have been observed in models of ice sheets (e.g., Lowry et al., 2020; Phipps et
 346 al., 2021; Pittard et al., 2022). Given the minimal impact of enhancement factors in this study, they were excluded from the
 347 Stage 2 sensitivity analysis.

348 When the T component parameters (subglacial water decay rate, maximum subglacial water thickness and bed friction angle)
 349 were varied between their minimum and maximum values (Fig. 3; Table 1) resulted in volume changes of -40.5% to +23.6%
 350 from their defaults across all domains. Minimum T parameter values increased basal sliding velocities substantially: up to
 351 +213.4% in the Copiapó (#4) domain (SI Fig. 12), a mean of +62.4% across all domains, leading to a mean ice thickness
 352 reduction of -20.9%. In contrast, maximum T parameter values reduced mean basal velocities by -49.2%, resulting in a mean
 353 thickness increase of +22.5% (Fig. 5). The resultant difference in the ice velocities and ice thicknesses can be seen in the shift

Commented [EL31]: RC2 - Line 269

354 of the ice divide, being primarily constrained to the glacier valley, to being more diffuse with minimal T component values,
 355 and being significant muted with maximum T component values.



356
 357 **Figure 5: An example of the influence of the subglacial component chosen parameters on the output of ice basal velocity in Vilcanota**
 358 **(#2) domain (Quelccaya Ice Cap). Remaining examples are shown in the Supplementary Information. Increased values of the chosen**
 359 **parameters generate reduced basal ice velocities, while decreasing values increase them. This can also lead to changes in ice divides**
 360 **as seen in T_min, compared to T_max. Values that correspond to 'max' and 'min' parameter values are found in Table 1.**

361 When the S component parameters (sliding exponent and velocity threshold) were varied between their minimum and
 362 maximum values (Table 1) resulted in ice volume changes of -43.2% to +41.2% (Fig. 3) from their defaults across all domains.
 363 Minimum S parameter values reduced basal velocities by a mean of -24.4% across all domains (-79.5% in the Copiapó
 364 domain), resulting in thicker ice (mean: +15.5%). Conversely, maximum values increased basal velocities by a mean of +47.7%
 365 (+235% in the Copiapó domain), leading to thinner ice with a mean of -17.3%. The larger percentage volume changes of the
 366 Copiapó domain reflect its low ice cover as small changes to the already small volume of ice (1.1 km³) yields large relative
 367 differences.

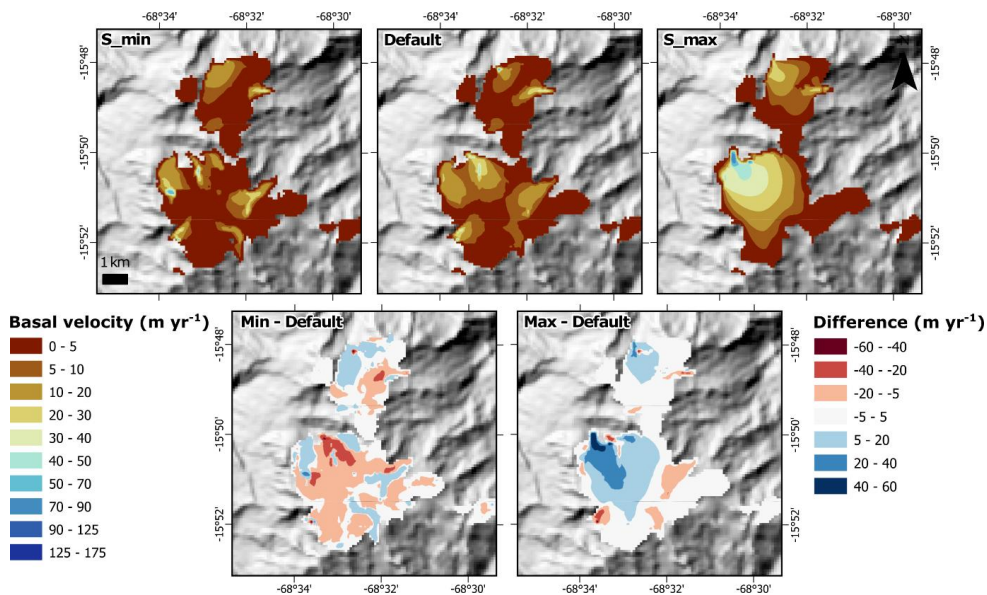


Figure 6: Example of the influence of sliding component parameters on basal ice velocity in the Kaka & Boopi (#3) domain (Ancohuma Ice Caps). Additional examples are provided in the Supplementary Information. Increased parameter values enhance basal velocities, while decreased values reduce them. Variations amplify or suppress sliding patterns already present in the default simulation. ‘Max’ and ‘min’ parameter values are listed in Table 1.

Collectively varying all parameters of the E, T, and S components between default, minimum, and maximum values (Table 1) produced a maximum mean ice volume increase of +109.3% across all five domains (Santa domain max: +247.2%), driven by the {E_min, T_max, S_min} combination (Fig. 3). The second highest mean increase of +89.3% (Santa domain max: +221.3%) resulted from {E_default, T_max, S_min}. Averaging across all combinations that include T_max or T_min produced mean ice volume changes of +33.6% and -22.6%, respectively, while those that include S_max or S_min produced changes of +38.6% and -23.2% respectively. Pearson correlation analysis (Table 4) confirms a strong and significant correlations ($p \leq 0.05$) for the T and S components and their effects on simulated ice volume in almost all domains.

Table 4: Pearson correlation statistics for all domains ($n = 27$ simulations per domain, 135 simulations overall) to understand the impact of model components on simulated ice volume. A value closer to zero (0) indicates a lower influence on the simulated volume output. A positive or negative number indicates that when the component value is varied it causes a gain or loss of simulated ice volume. The final row reports the mean absolute Pearson correlation across domains and is intended only as a descriptive summary of relative parameter influence, not as a formal regional

385 *statistic. These are then averaged, using their absolute values to show the overall influence across all domains.* * = $p \leq$
 386 **0.05**, ** = $p \leq 0.01$.

Domain	E	T	S
<i>Pearson correlation</i>	<i>Volume</i>	<i>Volume</i>	<i>Volume</i>
Santa	-0.16	0.47*	-0.39*
Vilcanota	-0.18	-0.36	0.51
Kaka & Boopi	-0.17	0.47*	-0.46*
Copiapó	-0.17	-0.46*	0.47*
Mendoza, Maipo & Rapel	-0.13	-0.49**	0.45*
<i>Mean absolute correlationAverage</i>	0.16	0.45	0.46

387
 388 Given its limited influence on simulated ice volume, the enhancement factors (E) with E_{SIA} and E_{SSA} parameters, is excluded
 389 from the individual parameter sensitivity analysis of Stage 2. The subglacial (T) and sliding (S) components demonstrated
 390 significant impacts through both univariate and multivariate perturbations and were included in the Stage 2 sensitivity
 391 experiments (Sect. 4.2).

392
 393 [Remarkably, between different domains the relative importance of parameters remains remarkably consistent \(Fig. 3\), although](#)
 394 [the magnitude of influence varies \(e.g. Table 4\). These intra-domain variations are likely an impact of different domain](#)
 395 [boundary conditions and settings. For instance, glacier size is likely to play a key role. The smallest domain, Copiapó, with](#)
 396 [also the smallest area of glacial ice, often showed large relative percentage changes because its default ice volume was small,](#)
 397 [meaning that modest absolute changes in ice thickness or extent produced proportionally large changes in model outputs.](#)
 398 [Conversely, larger and more glacierised domains, such as the Mendoza, Maipo, and Rapel domain, provided a broader range](#)
 399 [of glacier geometries and flow dynamics, producing a more complicated response to parameter perturbations. Climatic setting](#)
 400 [may also have influenced the magnitude of area and volume change for different parameter sets. Further work, varying the](#)
 401 [climate input for a given domain, is required to explore any potential interaction between ice flow parameters and climatic](#)
 402 [variables.](#)

404 4.2 Stage 2 – Individual parameter sensitivity analysis

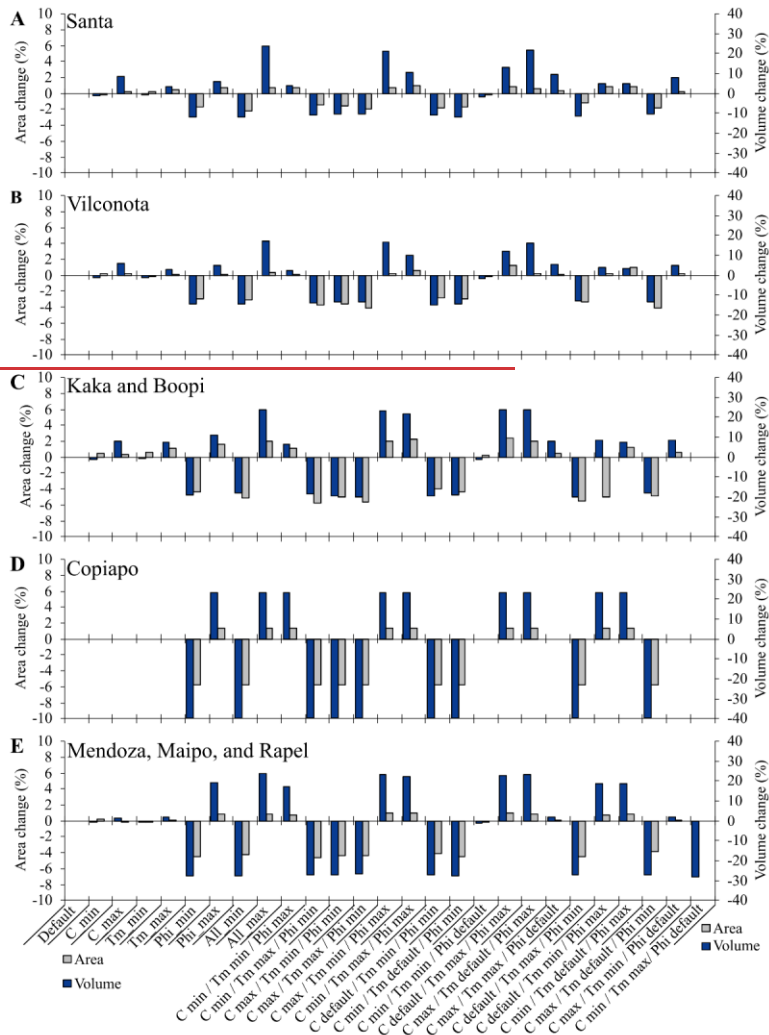
405 4.2.1 Subglacial model parameters (T Component)

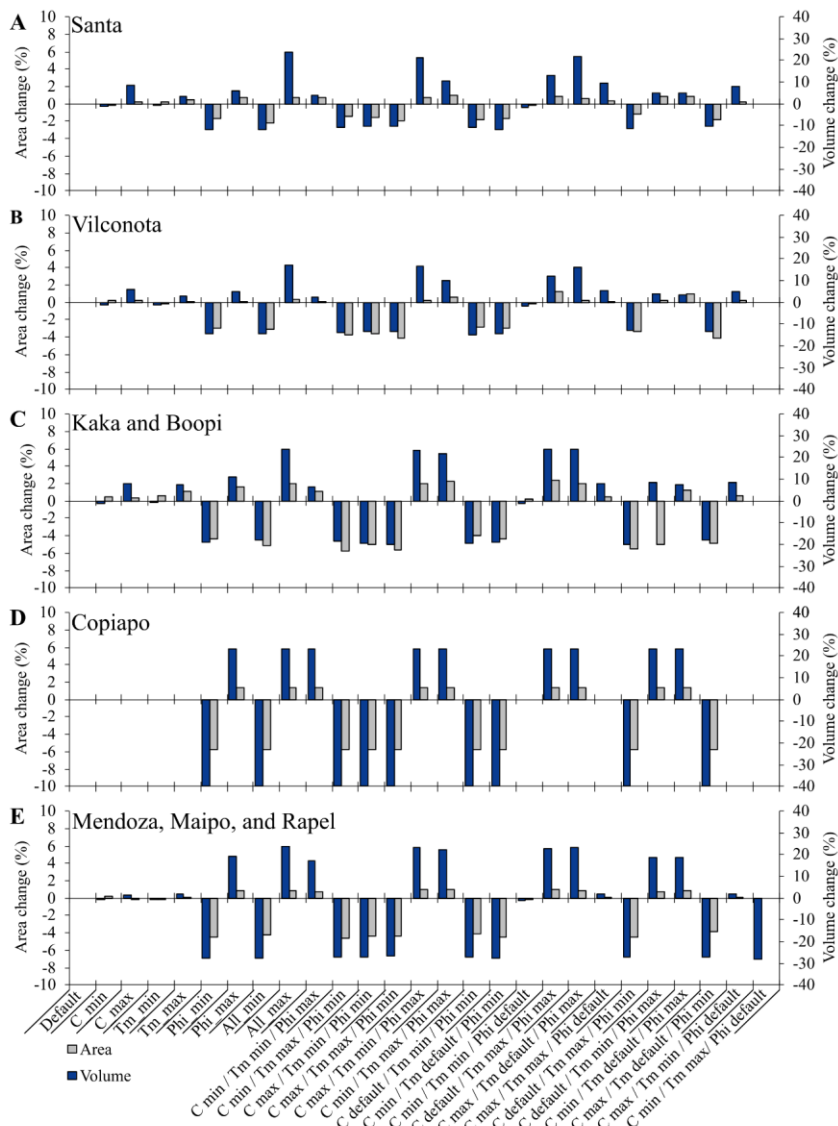
406 The T component parameter tests investigated the subglacial water decay rate (C), the maximum thickness of subglacial water
 407 (W_{till}^{max}), and basal friction angle (ϕ). Summary statistics for the T component tests are presented in Table 5 and Fig. 7. Among

408 all domains when the parameters were varied, the Copiapó domain, being the smallest, exhibited the largest change in simulated
 409 ice volume (-40.5%). The second largest change (+28.3%) occurred in the Mendoza, Maipo and Rapel domain, the largest and
 410 most ice-rich domain.

411 **Table 5: Overall, subglacial sensitivity analysis outputs detailing the default model simulation volume, and the maximum absolute**
 412 **percentage changes for volume for each domain across all the model simulation when components were varied between their**
 413 **maximum and minimum values.**

Domain	Volume (km ³)			Max abs change (%)
	Default	Max	Min	
Santa	10.1	12.5	8.95	23.6
Vilcanota	3.1	3.6	2.6	17.2
Kaka & Boopi	2.2	2.7	1.8	23.6
Copiapó	1.1	1.4	0.7	40.5
Mendoza, Maipo & Rapel	17.6	21.8	12.6	28.3





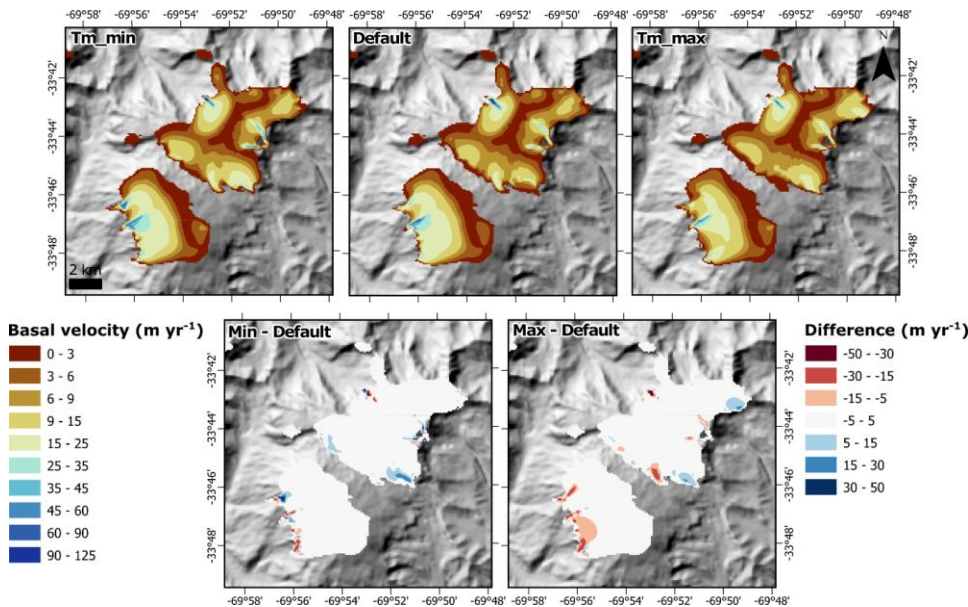
416 Figure 7: T sensitivity analysis detailing the area (grey) and volume (blue) absolute percentage changes due to changing the model
417 component parameters all together, for each of the five model domains. Blue and grey lines denote the default volume and area
418 respectively for comparison. Where there is no bar present for the component parameter, there was no change (0%). Subglacial
419 parameters are, C = basal water decay rate, $T_m = W_{till}^{max}$, $\Phi = \phi$. See Fig. 1 for domain locations.

420 Varying the subglacial water decay rate (C) between its minimum and maximum values (Table 1) resulted in ice volume
421 changes of -1.4% to +8.6% respectively across most domains. No change was observed in the Copiapó domain. This may
422 reflect the small glacierised area within this domain, where changes in subglacial hydrological parameters have limited
423 influence on domain-mean outputs. It may also reflect the simplified representation of subglacial hydrology in PISM, which
424 may not fully resolve hydrological variability beneath small mountain glaciers at the model resolution used here. No change
425 was observed in the Copiapó domain, likely due to the small size of its glacial ice, or due to PISM's simplified hydrology model
426 not able to affect the small glaciers due to the model resolution. Ice thickness and basal velocity changes across all domains
427 were minor or negligible (e.g., no change in the Copiapó domain, Fig. SI 25). Minimum C values slightly reduced ice
428 thicknesses (mean: -1.0%) and increased velocities (mean: +1.6%, -7.5% in the Vilcanota domain). Maximum C values
429 increased thickness (mean: +5.1%) and decreased velocities (mean: -14.6%), reflecting the larger deviation of the maximum
430 (12 mm/a) from the default (1 mm/a) relative to the minimum (0.1 mm/a).

431 When W_{till}^{max} was varied between its minimum and maximum values (Table 1), it resulted in ice volume changes of between -
432 1.0% to +7.7% across all domains (Fig. 7). No changes were seen across the Copiapó domain. Minimum W_{till}^{max} saw minimal
433 reductions in ice thickness (mean: -0.2%) and increases in velocity changes (mean: +3.3%), while maximum W_{till}^{max} provided
434 slightly increased ice thickness (mean: +2.5%) and reduced ice velocity (-6.6%) across all domains (Fig. 8). A stronger
435 reduction of -13.1% in ice velocity was identified in the Vilcanota domain with minimum W_{till}^{max} values. This may indicate
436 that, in this domain, reducing the maximum till water thickness, and thus the water storage, slightly increased basal resistance
437 in parts of the glacier bed where sliding occurs. However, the response remains small relative to the effects of the till friction
438 angle (detailed below) inferred to be related to the domain geometry or resolution effects within this region.

Commented [EL32]: RC1 - Lines 335-337

Commented [EL33]: RC2 - Line 347



439

440 **Figure 8:** An example of the influence of the W_{till}^{max} (Tm in Fig. panels) parameter on the output of ice basal velocity in the Mendoza,
 441 Maipo, and Rapel (#5) domain (Volcán Marmolejo). Remaining examples are shown in the Supplementary Information. Increased
 442 values the Tm parameter generally sees no, or very little changes in basal ice velocities. Values that correspond to ‘max’ and ‘min’
 443 parameter values are found in **Table 1**.

444 The parameters W_{till}^{max} and C had minimal, to no, impact on simulated ice outputs across all domains (Fig. 7). Similar minor
 445 effects of W_{till}^{max} over other valley glacier modelling efforts were reported by Candaş et al. (2020) and Žebre et al., (2021),
 446 although they saw greater sensitivity in their output than in our study due to W_{till}^{max} being varied in conjunction with the till
 447 effective fraction overburden (δ). No PISM-based studies to our knowledge have assessed sensitivity to C for valley glaciers.

448 However, variations in C have been shown to have an increased influence over ice sheets settings. Albrecht et al. (2020)
 449 details that increasing C from 1 to 10 mm yr⁻¹ can cause PISM to simulate an additional 11 m sea level equivalent (SLE) of
 450 meltwater from the Antarctic Ice Sheet over multiple glacial cycle timescales. This increasing-stronger influence over-in ice
 451 sheets settings is likely due to the greater role of subglacial hydrology in driving glacial-motion-and-ice streaming, influencing
 452 basal resistance and therefore ice discharge (Kazmierczak et al., 2022; Verjans and Robel, 2024). While subglacial hydrology
 453 does not affect valley-mountain glaciers to the same extent (Mair et al., 2002), they can affect glacier motion on diurnal time
 454 scales (Nienow et al., 2005) which would make modelling their interaction difficult. Our results indicate that these specific
 455 subglacial hydrology parameters have a limited impact on modelled ice outputs in our PISM simulations and can be removed

Commented [EL34]: RC1 - Line 362

Commented [EL35]: RC2 - Line 357

456 from future sensitivity analysis. This may reflect the model resolution used here, that may limit the influence of local basal-
457 topographic variability on sliding behaviour, or the use of the simplified representation of a non-conserving subglacial
458 hydrology (see Sect. 3.1.2) in PISM when applied to small mountain glaciers. Alternative PISM hydrology schemes, such a
459 steady flow or routing model, may produce stronger sensitivity in small, steep glacier catchments, allowing it to better represent
460 the subglacial hydrology.

Commented [EL36]: RC1 - Lines 363-365

461 Our results indicate limited impact from these specific parameters in PISM, that are likely due to either, an insufficient model
462 resolution, the basal topography not being sufficient to majorly affect basal sliding, or that the PISM hydrology is too simplistic
463 to accurately represent its effect over mountain glaciers. Neither parameter significantly affected valley glacier simulations in
464 our PISM ensemble. These parameters can likely be excluded from future valley glacier sensitivity analyses.

465 When ϕ was varied between its minimum and maximum values (Table 1), simulated ice volumes were saw changes between
466 -40.5% with minimum values and up to +23.4% with maximum values across the all domains, respectively. Minimum values
467 of ϕ led to substantial reductions in ice thickness (mean: -24.5%) due to increases in ice velocity (mean: +81.9%), while
468 maximum ϕ values led to increases in ice thickness (mean: +19.3%) and reductions in ice velocities (mean: -23.3%) (Fig. 9).
469 The most extreme differences were seen in the Copiapó domain, due to the region incurring the smallest glacier area, and any
470 changes can lead to larger relative (%) changes. The values above represent the domain-mean responses. Spatially, the velocity
471 response to ϕ -variations in ϕ are not uniform. Although increasing ϕ reduced mean basal velocity across the domains, localised
472 increases in basal velocity occurred in some areas (see Fig. 9 Phi_max). These localised increases likely reflect redistribution
473 of ice flow where changes in basal resistance altered glacier stress balance. Similarly, while reducing ϕ increased domain-
474 mean basal velocity, localised decreases occurred in some areas, likely due to redistribution of flow towards faster-flowing
475 parts of the glacier system.

Commented [EL37]: RC2 - Line 367

Commented [EL38]: RC2 - Line 368

Commented [EL39]: RC2 - L375

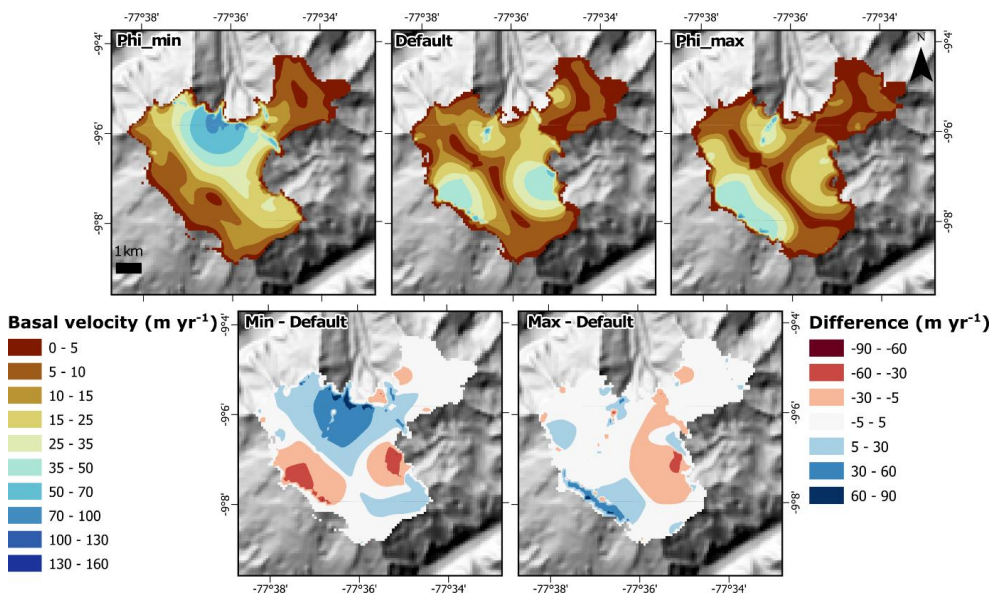


Figure 9: An example of the influence of the ϕ (Phi in Fig. panels) parameter on the output of ice basal velocity in the Santa (#1) domain (Huascarán Ice Cap). Remaining examples are shown in the Supplementary Information. Increased values of the ϕ parameter see a domain mean reduction in basal velocities, while the opposite is seen for decreased values, however there are localised increases and decreases in velocities with higher and lower ϕ reflect localised redistribution of ice flow. Values of 'max' and 'min' parameter values are in [Table 1](#).

Among the T component parameters, ϕ accounted for the greatest variance in simulated ice volume ([Table 7](#)), with a consistent influence across all domains ([Fig. 7](#)). Due to ϕ representing how resistant the subglacial sediment is to shear deformation, lower values represent wet fine sandy sediments promoting more basal motionsliding, while high values represent coarser dry gravels, or bedrock, reducing basal motionsliding ([Koloski et al., 1989; Cuffey and Paterson, 2010](#)). This therefore led to decreased domain-mean subglacial slidingvelocities, with higher values of ϕ leading to overall thicker ice (see *Phi_max* in [Fig. 9](#)), while lower values of ϕ increasing basaldomain-mean velocities leading to overall thinner ice (see *Phi_min* in [Fig. 9](#)). The influence of ϕ over the ice basal velocities is consistent with the intuitive nature of increased values of ϕ increasing basal resistance and thus limiting basal sliding. However, the response was not uniform spatially also yielded changes inwith ice basal velocities presenting the opposite to the domain-mean pattern within localised areas (i.e., increase ϕ seeing increase localised velocities and vice versa). These are likely due to changes in the ice divides and flow regimes that can lead to subsequent changes in the ice thicknesses and ice velocity. This localised vs domain-mean effect of the ϕ is consistent with previous studies showing that, even when using spatial uniform parameters, there can still be spatially variable basal conditions.

Commented [EL40]: RC1 - Lines 378-380

494 that can strongly influence velocity structure and sliding patterns across the model domain (Gowan et al., 2023; Johnson et al.,
 495 2023). In comparison with other studies, dynamics across the domain (see *Min–Default* in Fig 9). While ϕ has not been
 496 explicitly varied in previous valley-mountain glacier studies, to our knowledge, when modelling ice sheets ϕ is a key control
 497 on ice volume and subsequent ice dynamics (Albrecht et al., 2020; Koldtoft et al., 2021; Lowry et al., 2020). For example,
 498 lower ϕ values saw a reduction in modelled LGM volumes of the Antarctic Ice Sheet leading to accelerated retreat, whereas
 499 higher ϕ values tended to overestimate present-day ice sheet thicknesses (Albrecht et al., 2020; Lowry et al., 2020). Our
 500 findings highlight its importance in mountain glacier settings. Though a uniform ϕ was used here, it likely varies with
 501 catchment-specific geology (Bareither et al., 2008; Clarke, 2018), suggesting future studies should tune ϕ regionally to improve
 502 accuracy in ice dynamics and volume simulations.

Commented [EL41]: RC2 - Line 375

503 When all T component parameters were varied between their minimum, default, and maximum values, simulated ice volume
 504 differed by up to +40.5% relative to the default simulation-s. Across all domains, ice volumes cluster into three distinct groups
 505 eantered-centred on the minimum, default, and maximum ϕ values, most clearly seen in the Copiapó domain (#4Figure 7 D)
 506 and the Mendoza, Maipo and Rapel (Fig. 7 E#5) domains (Fig-7). While ϕ exerts dominant control over ice volumes, C and
 507 $W_{\text{till}}^{\text{max}}$ cause only minor variations within these groups. The highest volumes occurred when ϕ and other subglacial parameters
 508 were set to their maximum values {All_max}. Pearson correlations (Table 6) confirm the strong overwhelming influence of ϕ
 509 on simulated ice outputs, with an average coefficient of 0.94 across all domains. Moreover, ϕ was the only subglacial parameter
 510 with a statistically significant effect ($p \leq 0.01$), underscoring its primary role in controlling model outputs in PISM.

Commented [EL42]: RC1 - Line 392

Commented [EL43]: RC1 - Line 393

Commented [EL44]: RC1 - Lines 393-395

511 Table 6: Pearson correlation statistics for all five model domains (n = 27 simulations per domain; 135 total) showing the influence
 512 of subglacial model parameters on simulated ice volume. The final row reports the mean absolute Pearson correlation across
 513 domains and is intended only as a descriptive summary of relative parameter influence, not as a formal regional statistic. Explanation
 514 of Pearson correlation values shown in Table 4. ** = $p \leq 0.01$.

Commented [EL45]: RC1 - Line 397-399

Domain	C	$W_{\text{till}}^{\text{max}}$	ϕ
<i>Pearson correlation</i>	<i>Volume</i>	<i>Volume</i>	<i>Volume</i>
Santa	0.36	0.11	0.88**
Vilcanota	0.26	0.12	0.93**
Kaka & Boopi	0.18	0.12	0.95**
Copiapó	0.00	0.00	1.00**
Mendoza, Maipo & Rapel	0.09	-0.04	0.96**
<i>Mean absolute correlationAverage</i>	0.18	0.08	0.94

515 Across both univariate and multivariate parameter tests, ϕ consistently exerted the strongest influence on model outputs among
 516 the subglacial parameters. This is due to its role in the Mohr–Coulomb criterion, which governs the pseudo-plastic sliding law
 517 and modulates basal resistance (Cuffey and Paterson, 2010). Higher ϕ values increase basal resistance, slowing ice flow and
 518 leading to thicker ice, thereby raising total ice volume while having limited effect on ice extent. This relationship is reinforced
 519 by the ‘all max’ scenario, which produced the thickest and highest volume ice across nearly all domains.

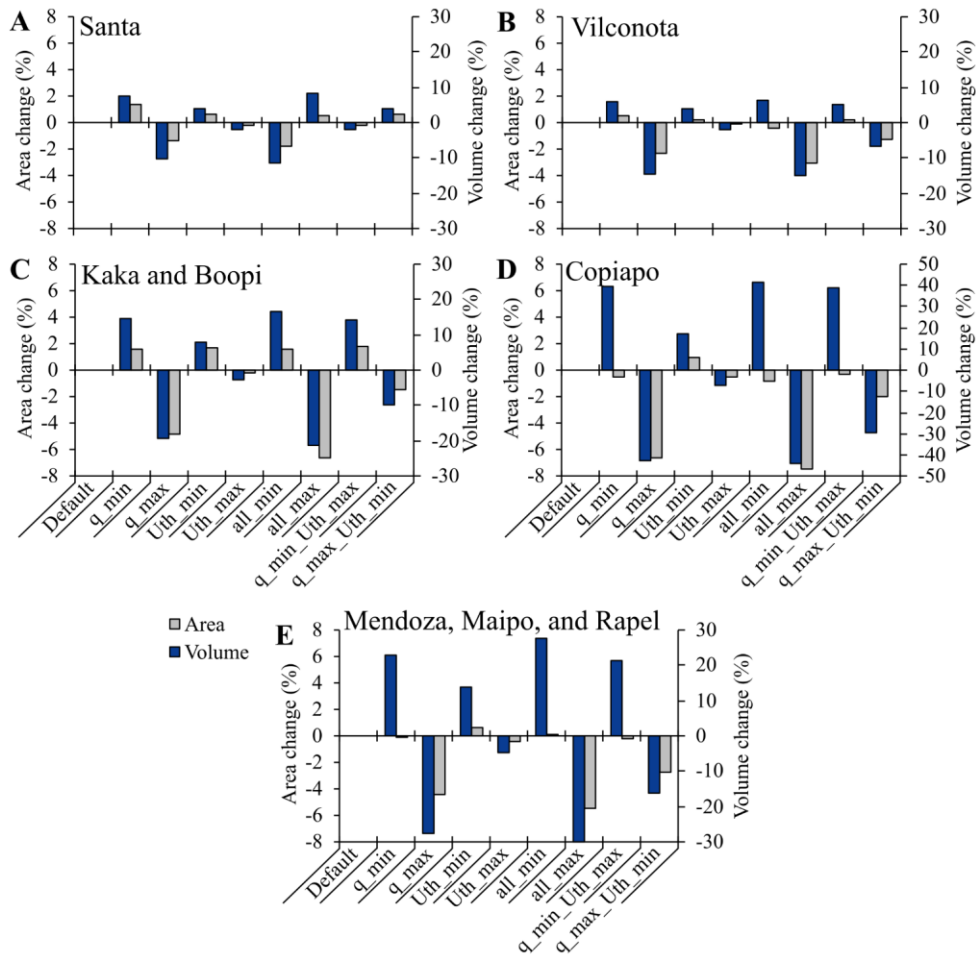
520

521 **4.2.2 Sliding model parameters (S Component)**

522 The S component tests focus on two parameters: the sliding exponent (q) and the velocity threshold ($uU_{threshold}$). Summary
 523 statistics for these tests are presented in [Table 7](#) and [Fig. 10](#). The PISM domains of Copiapó and Mendoza, Maipo and Rapel,
 524 representing the smallest and largest glaciers respectively, display the most pronounced responses to parameter variation, with
 525 maximum ice volume changes of 44.1% and 30.0%, respectively.

526 **Table 7: Sliding sensitivity analysis outputs detailing the default model simulation area and volume, and the maximum absolute**
 527 **percentage changes for ice volume for each domain across all the simulations when components were varied between their maximum**
 528 **and minimum values.**

Domain	Volume (km ³)			Max abs change (%)
	Default	Max	Min	
Santa	10.1	11.0	9.0	11.4
Vilcanota	3.1	3.3	2.6	14.9
Kaka & Boopi	2.2	2.6	1.7	21.4
Copiapó	1.1	1.6	0.6	44.1
Mendoza, Maipo & Rapel	17.6	22.5	12.3	30.0



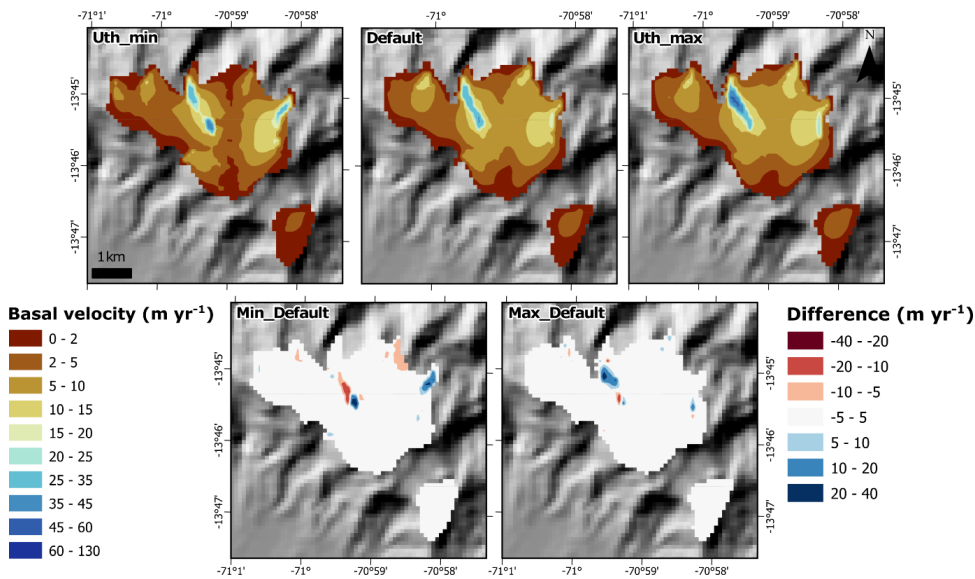
529
530
531
532
533

Figure 10: Sliding sensitivity analysis detailing the area (grey) and volume (blue) changes due to changing the model component parameters all together, for each of the five model domains. Blue and grey lines denote the default volume and area respectively for comparison. See Fig. 1 for domain locations. Note the change in y-axis in D), due to larger volume changes occurring in the Copiapo catchment, the catchment with the smallest ice area.

534
535

When $uU_{threshold}$ was varied between its minimum and maximum values (Table 1) produced ice volume differences of +17.1% to -7.2% respectively, with an absolute average difference of 6.5%. Across all domains minimum $U_{threshold}$ saw

536 increased ice thicknesses (mean: +9.1%) and basal velocities (mean: -19.2%) (Fig. 11). Maximum $U_{threshold}$ saw reduced ice
 537 thicknesses (mean: -3.7%) along with increased basal ice velocities (mean: +7.8%).

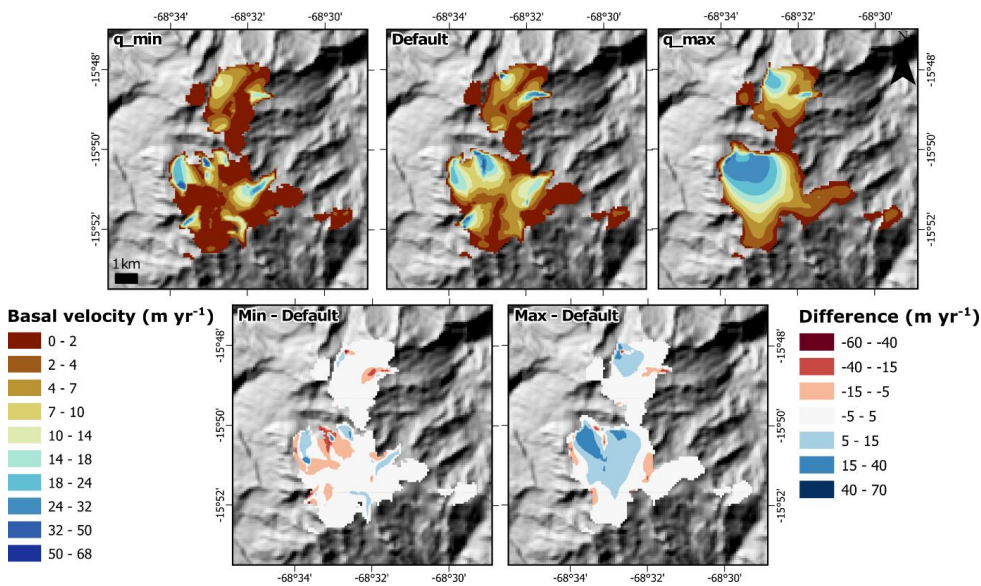


538
 539 **Figure 11:** An example of the influence of the $uU_{threshold}$ (U_{th} in Fig. panel) parameter on the output of ice basal velocity in the
 540 Vilcanota (#2) domain (Quelccaya Ice Cap). Remaining examples are shown in the Supplementary Information. An increase in the
 541 $uU_{threshold}$ parameter sees increased basal velocities, while the opposite is seen when values are decreased. Values that correspond
 542 to 'max' and 'min' parameter values are found in Table 1.

543 Variations of the $uU_{threshold}$, which controls the onset of basal sliding, leads to when the $U_{threshold}$ is set to lower values, ice
 544 flow velocities are decreased, increasing ice thickness and volume. However, while overall flow patterns remain very similar,
 545 their intensity shifts with varied $uU_{threshold}$ values. As can be seen in Fig. 11, with decreased $U_{threshold}$ values overall mean
 546 velocities decreased, but small localised areas of increased velocities (~ 10 to 20 m yr^{-1}) are seen where in the default run saw
 547 lower velocities occurred. When the $uU_{threshold}$ is increased, overall mean velocity increased, with areas of already faster
 548 flowing ice saw an increase in velocity ($\sim 20 \text{ m yr}^{-1}$), with locations of localised slower velocities remaining the same as those
 549 in the default. This behaviour is in line with the expected behaviour described in Sect. 3.1.3, whereby increases in the $u_{threshold}$
 550 delaying the transition to Coulomb-limited sliding that facilitates faster flowing ice. Despite this influence, $uU_{threshold}$ is rarely
 551 tested in mountain glacier modelling, with most studies using a fixed 100 m yr^{-1} value (Martin et al., 2022; Seguinot et al.,
 552 2014, 2018). Our results, spanning 20 to 200 m yr^{-1} , show that $uU_{threshold}$ meaningfully affects modelled dynamics and should
 553 be included in future sensitivity analyses.

Commented [EL46]: RC2 - Line 433

554 When q was varied between its minimum and maximum values (Table 1), it produced a difference in the ice volume between
 555 +39.6% and -42.3%, with an absolute average difference of 20.4%. The two largest differences in ice volume detailed before
 556 were all seen in the smallest domain of Copiapó (-42.3%), the second highest difference is seen in Mendoza, Maipo, and Rapel
 557 domain (-27.7%), both when q is set to its maximum value. Across all domains when q was set to its minimum, there was an
 558 increase in ice thickness (mean: +18.9%) and a decrease in ice velocity (mean: -33.6%), when set to its maximum there was a
 559 decrease in ice thickness (mean: -21.7%) and an increase in ice velocity (mean: +75.5%) (Fig. 12).



560

561 **Figure 12: An example of the influence of the sliding exponent (q) parameter on the output of ice basal velocity in the Kaka & Boopi**
 562 **(#3) domain (Ancohuima ice caps). Remaining examples are shown in the Supplementary Information. An increase or decrease in**
 563 **values of the q parameter see almost no effect in basal velocities. Values that correspond to 'max' and 'min' parameter values are**
 564 **found in Table 1.**

565 Variations of q within PISM exert a clear influence on simulated ice dynamics, due to its role in controlling the non-linearity
 566 of the basal sliding law (Zoet and Iverson, 2020). Higher q values suppress fast-flowing regions (e.g., $>25 \text{ m yr}^{-1}$) but enhance
 567 sliding in slower-flowing regions, producing a more diffuse velocity field (see q_{max} in Fig. 12). In contrast, lower q values
 568 concentrate flow into narrow corridors, altering ice divides and increasing ice thickness in surrounding slower-flow regions
 569 by limiting basal sliding (see q_{min} in Fig. 12). Among PISM studies, q is the most frequently varied sliding parameter,
 570 however, this in within the context of using the default Coulomb sliding model. Using the Coulomb sliding model Candaş et

571 al. (2020) over valley glaciers found that varying q altered ice volume by +22.6% at $q = 0$ and -26.4% at $q = 1$. In ice sheet
572 contexts, effects are mixed with Albrecht et al. (2020) reporting lower q reduced velocity and increased Antarctic volume at
573 the LGM by up to ± 3 m SLE. Over Greenland, Aschwanden et al. (2019) shows that the variance of q parameterization of 0.25
574 to 1.0 can lead to uncertainties on SLE contributions of 26-53% by 2100, 5-38% by 2200, and 2-33% by 2300. While the Zoet
575 and Iverson (2020) slip law has been not used by other PISM modelling studies, no study to have used the slip law within ice
576 sheet models (e.g., CISM; van den Akker et al., 2025) varied the parameterisation of the sliding exponent extensively. Our
577 findings here support the previous conclusion that q significantly affects modelled ice volumes, particularly in regions
578 dominated by valley-confined dynamic flow (see Section 4.2.2). The results, at least for q are the first to be presented using
579 the Zoet and Iverson (2020) slip law. We therefore recommend that future valley glacier modelling studies, especially those
580 focused on mass change, include q in their sensitivity analyses.

581 When q and $uU_{threshold}$ are varied together between their default, minimum, and maximum values, the largest ice volume
582 difference from the default simulation reaches -44.1%, observed in the Copiapo catchment (Fig. 10). Excluding this smallest
583 domain, the maximum difference is -30.0% in the Mendoza, Maipo and R domain. While q alone exerts the strongest influence,
584 combining both parameters amplifies their effects {All_max}. This is particularly evident when both are set to their minimum
585 or maximum values, resulting in greater or lesser increases in ice volume than when varied individually.

586 The Pearson correlation analysis (Table 8) confirms q as the dominant control on sliding-related sensitivity, with strong
587 correlations across nearly all domains except in the Santa catchment. Although the number of combined simulations is limited,
588 $U_{threshold}$ still produces noticeable changes in simulated outputs (Fig. 11), but its influence remains secondary to q when both
589 are varied simultaneously. This is likely because they both alter ice velocities, making it easier or more difficult for sliding to
590 occur. This supports that these two parameters should continue to be investigated by future model efforts over mountain
591 glaciers.

592 **Table 8: Pearson correlation statistics for all five model domains (n = 9 simulations per domain; 45 total) showing the influence of**
593 **sliding model parameters on simulated ice volume. The final row reports the mean absolute Pearson correlation across domains and**
594 **is intended only as a descriptive summary of relative parameter influence, not as a formal regional statistic. Explanation of Pearson**
595 **correlation values shown in Table 4. ** = $p \leq 0.01$.**

Domain	q	$uU_{threshold}$
Pearson correlation	Volume	Volume
Santa	0.13	0.16
Vilcanota	-0.90**	-0.25
Kaka & Boopi	-0.94**	-0.24
Copiapó	-0.94**	-0.17
Mendoza, Maipo & Rapel	-0.93**	-0.24
<i>Mean absolute correlation-Average</i>	-0.72	-0.15

596

597
598

4.3 Implications and recommendations for future work

599 The findings here using PISM suggest the less influential parameters ~~– the SIA and SSA enhancement factors (E_{SIA}), the till~~
600 ~~water decay rate (C), and the maximum till water thickness (W_{till}^{max}) – mention previously can may~~ be excluded from future
601 sensitivity ensembles or parameter optimisation simulations, at least for Andean Mountain glaciers under climates close to
602 present day. This aligns with findings from other PISM-based studies in other contexts (e.g., Albrecht et al., 2020; Candaş et
603 al., 2020; Žebre et al., 2021), which similarly report minimal differences in modelled outputs when E_{SIA} , E_{SSA} , W_{till}^{max} , q , and C
604 are varied within reasonable bounds. Their exclusion offers the potential to streamline future modelling efforts on their
605 parameter perturbation selection, reducing computational demands and enabling more efficient ensemble designs. This enables
606 researchers to allocate computational resources toward exploring more influential parameters in greater depth or across broader
607 ranges, such as till friction angle, sliding exponent, and the velocity threshold.

608 ~~Further,~~ Future work should examine parameters and model choice that have not been explored here. Some parameters in
609 PISM have historically been left as ‘model defaults’ and unchanged, based on physical assumptions or field data derived from
610 non-valley glacier environments (or continental scale ice studies), limiting their applicability. Additionally, many parameters
611 have not been explored in-detail within PISM for valley glaciers which, with the reduction in potential parameters to be
612 perturbed presented here, can now be focused on. For example, future work could examine the impact of subglacial hydrology
613 model choices, such as the difference between mass-conserving routing models and the non-conserving null model used here
614 on valley glacier dynamics. Another example of future work can be examining the difference in the number of vertical layers
615 within the chosen model domain. While a lower number of layers decreases computation time, and vice versa, this factor has
616 not been studied in detail to understand how vertical grid resolution impacts basal thermal regimes, ice flow, and the overall
617 model output over mountain glaciers.

618 Results from this study demonstrate that ice flow parameters influence simulated ice volume, while for ice area it is mainly
619 unaffected. For applications related to water resources, such as runoff or meltwater estimates, understanding the internal ice
620 physics and associated parameter sensitivities on ice volume is essential to understand how much ice (or water) remains in the
621 future. However, studies that focus on glacier area, or are lacking robust ice volume constraints, should prioritise sensitivity
622 analysis for climatic parameters; in particular, those ~~using that effect~~ PDD model. ~~sAs shown in previous study,~~ for transient
623 simulations, climatic parameters such as degree day factors snow and ice will likely find that climatic parameters exert the
624 strongest control over both ice area and volume (e.g., Martin et al., 2022). ~~Further,~~ PISM has also added the new diurnal energy
625 balance model simple (dEBM-simple) that improves upon the PDD model by accounting for melt-albedo feedback and
626 shortwave radiation, without a significant increase in computational time (Zeitl et al., 2021). This model has only been applied

Commented [EL47]: RC1 - Lines 481-482

Commented [EL48]: RC1 - Lines 184-185

627 in ice sheet settings but may better represent climatic interactions over mountain glaciers given its explicit consideration of
628 radiative melting.

Commented [EL49]: RC1 - Lines 497-500

630 5 Conclusion

631 This study investigated the influence of internal ice flow parameters within PISM over valley glaciers across our five Andean
632 domains (8 hydrological catchments) in South America. We examined parameters previously tested in smaller-scale previous
633 studies, and others that have either identified parameters as having a large influence over, or having mixed influence, influential
634 over ice model outputs, in different glacial environments. By applying these tests across multiple domains of varying sizes,
635 we evaluated whether sensitivity differed with glacier scale. While the smallest (Copiapó) and largest (Mendoza, Maipo and
636 Rapel) model domains, with the least and most ice respectively, exhibited the most pronounced volume differences, the overall
637 response to parameter perturbations was relatively consistent across all domains.

Commented [EL50]: RC2 - Line 505

638 Of the components assessed, the enhancement factors showed the least sensitivity, producing the least difference in ice volume.
639 Within the subglacial component, the parameters C and W_{till}^{max} saw negligible impact on modelled ice outputs. We therefore
640 suggest that further testing of these parameters is unnecessary for similar valley glacier modelling applications in PISM,
641 especially under climate and glacier conditions close to present day.

642 The sliding component parameters of the velocity threshold ($U_{threshold}$) and sliding exponent (q), exhibited moderate influence
643 over ice volume. While both impacted ice thickness and velocity, q had the dominant influence when the sliding component
644 parameters were perturbed together. Within the till component, the greatest overall control on simulated ice volume came from
645 the till friction angle (ϕ). This saw the largest differences produced in ice thickness and basal velocities. This underscores the
646 dominant role of basal conditions in valley glacier dynamics within PISM and a parameter that should see further investigation
647 within modelling studies.

648 Unlike most previous PISM sensitivity studies, which have focused on ice sheets or limited mountain glacier domains, this
649 study systematically examined the influence of internal ice dynamics on valley glaciers in the Andes. Our findings reinforce
650 the need for detailed investigation of subglacial-related parameters, especially basal resistance (ϕ). We also detail continued
651 support for the investigation of the sliding exponent (q), at least within the Zoet and Iverson (2020) slip law, which was recently
652 implemented into PISM and has not been varied before this study. We also recommend that future studies explore the role of
653 subglacial hydrology models, such as the choice between mass-conserving and non-conserving schemes, and their potential
654 influence on modelled glacier behaviour, and just how this influence may be affected by model resolution.

655 This work represents the first stage in the glacier modelling workflow of the *Deplete and Retreat* project. The insights gained
656 here will directly inform the design of a Latin Hypercube ensemble by eliminating parameters with negligible impact, thereby

657 refining the efficiency and robustness of subsequent simulations. Our results can inform future sensitivity analyses and
658 optimisation studies for glacier and ice sheet models, enabling researchers to prioritise parameters with substantial impacts on
659 model outputs and avoid testing those with minimal influence. This efficiency can help conserve computational resources
660 while guiding more targeted investigations into parameter effects on modelled ice outputs.

661

662 *Supplementary Information.* Extra information on ice metrics can be found within the Supplementary Information, along with
663 extra figures that detail ice outputs from each domain. An example of the scripts used to conduct the modelling are available
664 at the <https://zenodo.org/records/17878115> DOI: [10.5281/zenodo.17878114](https://doi.org/10.5281/zenodo.17878114).

665

666 *Competing Interests.* The authors declare that they have no conflict of interest.

667

668 *Author Contributions.* JE and EL conceptualised the study. EL collated the model input data and conducted the numerical
669 modelling for the study. EL and JE analysed the model output. EL wrote the first draft. Manuscript comments and edits were
670 provided by all authors.

671

672 *Financial Support.* This work was part of the Natural Environment Research Council (NERC) highlight topic grant “Deplete
673 and Retreat: the future of Andean Water Towers” (NE/X004031/1).

674

675 *Acknowledgements.* We acknowledge the IT Services at the University of Sheffield for the provision of services for High
676 Performance Computing which was used to conduct numerical modelling in this study.

677

678 References

679 van den Akker, T., Lipscomb, W. H., Leguy, G. R., Bernales, J., Berends, C. J., van de Berg, W. J., and van de Wal, R. S.
680 W.: Present-day mass loss rates are a precursor for West Antarctic Ice Sheet collapse, *The Cryosphere*, 19, 283–301,
681 <https://doi.org/10.5194/tc-19-283-2025>, 2025.

682 Albrecht, T., Winkelmann, R., and Levermann, A.: Glacial-cycle simulations of the Antarctic Ice Sheet with the Parallel Ice
683 Sheet Model (PISM) – Part 1: Boundary conditions and climatic forcing, *The Cryosphere*, 14, 599–632,
684 <https://doi.org/10.5194/tc-14-599-2020>, 2020.

Commented [EL51]: RC1 - Line 535

- 685 Archer, R.: Bayesian inference to calibrate flow geometry in ice sheet modelling of the last Scandinavian Ice Sheet,
686 University of Sheffield, 2024.
- 687 Aschwanden, A., Aðalgeirsdóttir, G., and Khroulev, C.: Hindcasting to measure ice sheet model sensitivity to initial states,
688 The Cryosphere, 7, 1083–1093, <https://doi.org/10.5194/tc-7-1083-2013>, 2013.
- 689 Aschwanden, A., Fahnestock, M. A., Truffer, M., Brinkerhoff, D. J., Hock, R., Khroulev, C., Mottram, R., and Khan, S. A.:
690 Contribution of the Greenland Ice Sheet to sea level over the next millennium, *Science Advances*, 5, eaav9396,
691 <https://doi.org/10.1126/sciadv.aav9396>, 2019.
- 692 Bareither, C., Edil, T., Benson, C., and Mickelson, D.: Geological and Physical Factors Affecting the Friction Angle of
693 Compacted Sands, *Journal of Geotechnical and Geoenvironmental Engineering*, 134, 1476–1489,
694 [https://doi.org/10.1061/\(ASCE\)1090-0241\(2008\)134:10\(1476\)](https://doi.org/10.1061/(ASCE)1090-0241(2008)134:10(1476)), 2008.
- 695 Berdahl, M., Leguy, G., Lipscomb, W. H., and Urban, N. M.: Statistical emulation of a perturbed basal melt ensemble of an
696 ice sheet model to better quantify Antarctic sea level rise uncertainties, *The Cryosphere*, 15, 2683–2699,
697 <https://doi.org/10.5194/tc-15-2683-2021>, 2021.
- 698 Bevan, S., Cornford, S., Gilbert, L., Otosaka, I., Martin, D., and Surawy-Stepney, T.: Amundsen Sea Embayment ice-sheet
699 mass-loss predictions to 2050 calibrated using observations of velocity and elevation change, *Journal of Glaciology*, 69,
700 1729–1739, <https://doi.org/10.1017/jog.2023.57>, 2023.
- 701 Bolibar, J., Rabatel, A., Gouttevin, I., Zekollari, H., and Galiez, C.: Nonlinear sensitivity of glacier mass balance to future
702 climate change unveiled by deep learning, *Nature Communications*, 13, 409, <https://doi.org/10.1038/s41467-022-28033-0>,
703 2022.
- 704 Bueler, E. and Brown, J.: Shallow shelf approximation as a “sliding law” in a thermomechanically coupled ice sheet model,
705 *Journal of Geophysical Research: Earth Surface*, 114, <https://doi.org/10.1029/2008JF001179>, 2009.
- 706 Buytaert, W., Moulds, S., Acosta, L., De Bièvre, B., Olmos, C., Villacis, M., Tovar, C., and Verbist, K. M. J.: Glacial melt
707 content of water use in the tropical Andes, *Environmental Research Letters*, 12, 114014, <https://doi.org/10.1088/1748-9326/aa926c>, 2017.
- 709 Byrne, M. P., Boos, W. R., and Hu, S.: Elevation-dependent warming: observations, models, and energetic mechanisms,
710 *Weather Clim. Dynam.*, 5, 763–777, <https://doi.org/10.5194/wcd-5-763-2024>, 2024.
- 711 Cai, W., McPhaden, M. J., Grimm, A. M., Rodrigues, R. R., Taschetto, A. S., Garreaud, R. D., Dewitte, B., Poveda, G.,
712 Ham, Y.-G., Santoso, A., Ng, B., Anderson, W., Wang, G., Geng, T., Jo, H.-S., Marengo, J. A., Alves, L. M., Osman, M., Li,
713 S., Wu, L., Karamperidou, C., Takahashi, K., and Vera, C.: Climate impacts of the El Niño–Southern Oscillation on South
714 America, *Nature Reviews Earth & Environment*, 1, 215–231, <https://doi.org/10.1038/s43017-020-0040-3>, 2020.
- 715 Calov, R. and Greve, R.: A semi-analytical solution for the positive degree-day model with stochastic temperature variations,
716 *Journal of Glaciology*, 51, 173–175, <https://doi.org/10.3189/172756505781829601>, 2005.
- 717 Candaş, A., Sarıkaya, M. A., KÖSE, O., Şen, Ö. L., and Çiner, A.: Modelling Last Glacial Maximum ice cap with the
718 Parallel Ice Sheet Model to infer palaeoclimate in south-west Turkey, *Journal of Quaternary Science*, 35, 935–950,
719 <https://doi.org/10.1002/jqs.3239>, 2020.
- 720 [Carrivick, J. L., and Heckmann, T.: Short-term geomorphological evolution of proglacial systems, *Geomorphology*, 287, 3–](https://doi.org/10.1016/j.geomorph.2017.01.037)
721 [28, <https://doi.org/10.1016/j.geomorph.2017.01.037>, 2017.](https://doi.org/10.1016/j.geomorph.2017.01.037)

- 722 Carrivick, J. L., Davies, M., Wilson, R., Davies, B. J., Gribbin, T., King, O., Rabatel, A., García, J.-L., and Ely, J. C.:
 723 Accelerating Glacier Area Loss Across the Andes Since the Little Ice Age, *Geophysical Research Letters*, 51,
 724 e2024GL109154, <https://doi.org/10.1029/2024GL109154>, 2024.
- 725 Clarke, B. G.: The engineering properties of glacial tills, *Geotechnical Research*, 5, 262–277,
 726 <https://doi.org/10.1680/jgere.18.00020>, 2018.
- 727 Cuffey, K. M. and Paterson, W. S. B.: Basal Slip, in: *The physics of glaciers*, edited by: Paterson, W. S. B., Butterworth-
 728 Heinemann, London, 223–284, 2010.
- 729 Cuzzone, J., Romero, M., and Marcott, S. A.: Modeling the timing of Patagonian Ice Sheet retreat in the Chilean Lake
 730 District from 22–10 ka, *The Cryosphere*, 18, 1381–1398, <https://doi.org/10.5194/tc-18-1381-2024>, 2024.
- 731 Davies, J. H.: Global map of solid Earth surface heat flow, *Geochemistry, Geophysics, Geosystems*, 14, 4608–4622,
 732 <https://doi.org/10.1002/ggge.20271>, 2013.
- 733 Drenkhan, F., Carey, M., Huggel, C., Seidel, J., and Oré, M. T.: The changing water cycle: climatic and socioeconomic
 734 drivers of water-related changes in the Andes of Peru, *WIREs Water*, 2, 715–733, <https://doi.org/10.1002/wat2.1105>, 2015.
- 735 Dussailant, I., Berthier, E., Brun, F., Masiokas, M., Hugonnet, R., Favier, V., Rabatel, A., Pitte, P., and Ruiz, L.: Two
 736 decades of glacier mass loss along the Andes, *Nature Geoscience*, 12, 802–808, <https://doi.org/10.1038/s41561-019-0432-5>,
 737 2019.
- 738 [Echelmeyer, K., and Zhongxiang, W.: Direct Observation of Basal Sliding and Deformation of Basal Drift at Sub-Freezing](#)
 739 [Temperatures, *Journal of Glaciology*, 33, 83–98, <https://doi.org/10.3189/S0022143000005396>, 1987.](#)
- 740 Edwards, T. L., Nowicki, S., Marzeion, B., Hock, R., Goelzer, H., Seroussi, H., Jourdain, N. C., Slater, D. A., Turner, F. E.,
 741 Smith, C. J., McKenna, C. M., Simon, E., Abe-Ouchi, A., Gregory, J. M., Larour, E., Lipscomb, W. H., Payne, A. J.,
 742 Shepherd, A., Agosta, C., Alexander, P., Albrecht, T., Anderson, B., Asay-Davis, X., Aschwanden, A., Barthel, A., Bliss, A.,
 743 Calov, R., Chambers, C., Champollion, N., Choi, Y., Cullather, R., Cuzzone, J., Dumas, C., Felikson, D., Fettweis, X.,
 744 Fujita, K., Galton-Fenzi, B. K., Gladstone, R., Golledge, N. R., Greve, R., Hattermann, T., Hoffman, M. J., Humbert, A.,
 745 Huss, M., Huybrechts, P., Immerzeel, W., Kleiner, T., Kraaijenbrink, P., Le clec'h, S., Lee, V., Leguy, G. R., Little, C. M.,
 746 Lowry, D. P., Malles, J.-H., Martin, D. F., Maussion, F., Morlighem, M., O'Neill, J. F., Nias, I., Pattyn, F., Pelle, T., Price,
 747 S. F., Quiquet, A., Radić, V., Reese, R., Rounce, D. R., Rückamp, M., Sakai, A., Shafer, C., Schlegel, N.-J., Shannon, S.,
 748 Smith, R. S., Straneo, F., Sun, S., Tarasov, L., Trusel, L. D., Van Breedam, J., van de Wal, R., van den Broeke, M.,
 749 Winkelmann, R., Zekollari, H., Zhao, C., Zhang, T., and Zwinger, T.: Projected land ice contributions to twenty-first-century
 750 sea level rise, *Nature*, 593, 74–82, <https://doi.org/10.1038/s41586-021-03302-y>, 2021.
- 751 Egholm, D. L., Knudsen, M. F., Clark, C. D., and Lesemann, J. E.: Modeling the flow of glaciers in steep terrains: The
 752 integrated second-order shallow ice approximation (iSOSIA), *Journal of Geophysical Research: Earth Surface*, 116,
 753 <https://doi.org/10.1029/2010JF001900>, 2011.
- 754 Ely, J. C., Clark, C. D., Bradley, S. L., Gregoire, L., Gandy, N., Gasson, E., Veness, R. L. J., and Archer, R.: Behavioural
 755 tendencies of the last British–Irish Ice Sheet revealed by data–model comparison, *Journal of Quaternary Science*,
 756 <https://doi.org/10.1002/jqs.3628>, 2024.
- 757 Emmer, A., Le Roy, M., Sattar, A., Veettil, B. K., Alcalá-Reygosa, J., Campos, N., Malecki, J., and Cochachin, A.: Glacier
 758 retreat and associated processes since the Last Glacial Maximum in the Lejiamayu valley, Peruvian Andes, *Journal of South*
 759 *American Earth Sciences*, 109, 103254, <https://doi.org/10.1016/j.jsames.2021.103254>, 2021.

760 Fick, S. E. and Hijmans, R. J.: WorldClim 2: new 1-km spatial resolution climate surfaces for global land areas, *International*
761 *Journal of Climatology*, 37, 4302–4315, <https://doi.org/10.1002/joc.5086>, 2017.

762 Flowers, G. E.: Modelling water flow under glaciers and ice sheets, *Proceedings of the Royal Society A: Mathematical,*
763 *Physical and Engineering Sciences*, 471, 20140907, <https://doi.org/doi:10.1098/rspa.2014.0907>, 2015.

764 Fox-Kemper, B., H. T. Hewitt, C. Xiao, G. Aðalgeirsdóttir, S. S. Drijfhout, T. L. Edwards, N. R. Golledge, M. Hemer, R. E.
765 Kopp, G. Krinner, A. Mix, D. Notz, S. Nowicki, I. S. Nurhati, L. Ruiz, J. -B. Sallée, A. B.A. Slangen, and Y. Yu, 2021:
766 Ocean, Cryosphere and Sea Level Change, in: *Climate Change 2021 – The Physical Science Basis: Working Group I*
767 *Contribution to the Sixth Assessment Report of the Intergovernmental Panel on Climate Change*, edited by: Masson-
768 Delmotte, V., P. Zhai, A. Pirani, S. L. Connors, C. Péan, S. Berger, N. Caud, Y. Chen, L. Goldfarb, M. I. Gomis, M. Huang,
769 K. Leitzell, E. Lonnoy, J. B.R. Matthews, T. K. Maycock, T. Waterfield, O. Yelekçi, R. Yu, and B. Zhou, Cambridge
770 University Press, Cambridge, 1211–1362, 2023.

771 Fyffe, C. L., Potter, E., Fugger, S., Orr, A., Fatichi, S., Loarte, E., Medina, K., Hellström, R. Å., Bernat, M., Aubry-Wake,
772 C., Gurgiser, W., Perry, L. B., Suarez, W., Quincey, D. J., and Pellicciotti, F.: The Energy and Mass Balance of Peruvian
773 Glaciers, *Journal of Geophysical Research: Atmospheres*, 126, e2021JD034911, <https://doi.org/10.1029/2021JD034911>,
774 2021.

775 Goelzer, H., Nowicki, S., Payne, A., Larour, E., Seroussi, H., Lipscomb, W. H., Gregory, J., Abe-Ouchi, A., Shepherd, A.,
776 Simon, E., Agosta, C., Alexander, P., Aschwanden, A., Barthel, A., Calov, R., Chambers, C., Choi, Y., Cuzzzone, J., Dumas,
777 C., Edwards, T., Felikson, D., Fettweis, X., Golledge, N. R., Greve, R., Humbert, A., Huybrechts, P., Le clec’h, S., Lee, V.,
778 Leguy, G., Little, C., Lowry, D. P., Morlighem, M., Nias, I., Quiquet, A., Rückamp, M., Schlegel, N. J., Slater, D. A., Smith,
779 R. S., Straneo, F., Tarasov, L., van de Wal, R., and van den Broeke, M.: The future sea-level contribution of the Greenland
780 ice sheet: a multi-model ensemble study of ISMIP6, *The Cryosphere*, 14, 3071–3096, [https://doi.org/10.5194/tc-14-3071-](https://doi.org/10.5194/tc-14-3071-2020)
781 [2020](https://doi.org/10.5194/tc-14-3071-2020), 2020.

782 Golledge, N. R., Mackintosh, A. N., Anderson, B. M., Buckley, K. M., Doughty, A. M., Barrell, D. J. A., Denton, G. H.,
783 Vandergoes, M. J., Andersen, B. G., and Schaefer, J. M.: Last Glacial Maximum climate in New Zealand inferred from a
784 modelled Southern Alps icefield, *Quaternary Science Reviews*, 46, 30–45, <https://doi.org/10.1016/j.quascirev.2012.05.004>,
785 2012.

786 Hardy, D. R., Vuille, M., Braun, C., Keimig, F., and Bradley, R. S.: Annual and Daily Meteorological Cycles at High
787 Altitude on a Tropical Mountain, *Bulletin of the American Meteorological Society*, 79, 1899–1914,
788 [https://doi.org/10.1175/1520-0477\(1998\)079%3C1899:AADMCA%3E2.0.CO;2](https://doi.org/10.1175/1520-0477(1998)079%3C1899:AADMCA%3E2.0.CO;2), 1998.

789 Hock, R., Bliss, A., Marzeion, B. E. N., Giesen, R. H., Hirabayashi, Y., Huss, M., Radić, V., and Slangen, A. B. A.:
790 GlacierMIP – A model intercomparison of global-scale glacier mass-balance models and projections, *Journal of Glaciology*,
791 65, 453–467, <https://doi.org/10.1017/jog.2019.22>, 2019.

792 Hoffman, A. O., Christianson, K., Holschuh, N., Case, E., Kingslake, J., and Arthern, R.: The Impact of Basal Roughness on
793 Inland Thwaites Glacier Sliding, *Geophysical Research Letters*, 49, e2021GL096564,
794 <https://doi.org/10.1029/2021GL096564>, 2022.

795 Hugonnet, R., McNabb, R., Berthier, E., Menounos, B., Nuth, C., Girod, L., Farinotti, D., Huss, M., Dussailant, I., Brun, F.,
796 and Kääb, A.: Accelerated global glacier mass loss in the early twenty-first century, *Nature*, 592, 726–731,
797 <https://doi.org/10.1038/s41586-021-03436-z>, 2021.

798 Hutter, K.: *The Application of the Shallow-Ice Approximation*, in: *Theoretical Glaciology: Material Science of Ice and the*
799 *Mechanics of Glaciers and Ice Sheets*, Springer Netherlands, Dordrecht, 256–332, 1983.

800 Immerzeel, W. W., Lutz, A. F., Andrade, M., Bahl, A., Biemans, H., Bolch, T., Hyde, S., Brumby, S., Davies, B. J., Elmore,
801 A. C., Emmer, A., Feng, M., Fernández, A., Haritashya, U., Kargel, J. S., Koppes, M., Kraaijenbrink, P. D. A., Kulkarni, A.
802 V., Mayewski, P. A., Nepal, S., Pacheco, P., Painter, T. H., Pellicciotti, F., Rajaram, H., Rupper, S., Sinisalo, A., Shrestha,
803 A. B., Viviroli, D., Wada, Y., Xiao, C., Yao, T., and Baillie, J. E. M.: Importance and vulnerability of the world's water
804 towers, *Nature*, 577, 364–369, <https://doi.org/10.1038/s41586-019-1822-y>, 2020.

805 Johnson, A., Aschwanden, A., Albrecht, T., and Hock, R.: Range of 21st century ice mass changes in the Filchner-Ronne
806 region of Antarctica, *Journal of Glaciology*, 69, 1203–1213, <https://doi.org/10.1017/jog.2023.10>, 2023.

807 Joughin, I., Shapero, D., and Dutrieux, P.: Responses of the Pine Island and Thwaites glaciers to melt and sliding
808 parameterizations, *The Cryosphere*, 18, 2583–2601, <https://doi.org/10.5194/tc-18-2583-2024>, 2024.

809 Kaser, G.: A review of the modern fluctuations of tropical glaciers, *Global and Planetary Change*, 22, 93–103,
810 [https://doi.org/10.1016/S0921-8181\(99\)00028-4](https://doi.org/10.1016/S0921-8181(99)00028-4), 1999.

811 Kazmierczak, E., Sun, S., Coulon, V., and Pattyn, F.: Subglacial hydrology modulates basal sliding response of the Antarctic
812 ice sheet to climate forcing, *The Cryosphere*, 16, 4537–4552, <https://doi.org/10.5194/tc-16-4537-2022>, 2022.

813 Khan, S. A., Choi, Y., Morlighem, M., Rignot, E., Helm, V., Humbert, A., Mougnot, J., Millan, R., Kjær, K. H., and Bjørk,
814 A. A.: Extensive inland thinning and speed-up of Northeast Greenland Ice Stream, *Nature*, 611, 727–732,
815 <https://doi.org/10.1038/s41586-022-05301-z>, 2022.

816 Koldtoft, I., Grinsted, A., Vinther, B. M., and Hvidberg, C. S.: Ice thickness and volume of the Renland Ice Cap, East
817 Greenland, *Journal of Glaciology*, 67, 714–726, <https://doi.org/10.1017/jog.2021.11>, 2021.

818 Koloski, J. W., Schwarz, S. D., and Tubbs, D. W.: Geotechnical Properties of Geologic Materials, in: *Engineering Geology*
819 *in Washington*, vol. 1, edited by: Galster, R. W., Washington Division of Geology and Earth Resources Bulletin,
820 Washington, 1989.

821 [Lee, E., Ross, N., Henderson, A. C. G., Russell, A. J., Jamieson, S. S. R., and Fabel, D.: Palaeoglaciacion in the Low](https://doi.org/10.3389/feart.2022.838826)
822 [Latitude, Low Elevation Tropical Andes, Northern Peru, *Frontiers in Earth Science*, 10, 838826,](https://doi.org/10.3389/feart.2022.838826)
823 [https://doi.org/10.3389/feart.2022.838826, 2022.](https://doi.org/10.3389/feart.2022.838826)

824 [Lee, E.: The frozen tropics: palaeoglaciacion within northern Peru, PhD thesis, Newcastle University, Newcastle upon Tyne,](http://theses.ncl.ac.uk/jspui/handle/10443/6555)
825 [UK, http://theses.ncl.ac.uk/jspui/handle/10443/6555, 2024.](http://theses.ncl.ac.uk/jspui/handle/10443/6555)

826 Lehner, B., Verdin, K., and Jarvis, A.: New Global Hydrography Derived From Spaceborne Elevation Data, *Eos*,
827 *Transactions American Geophysical Union*, 89, 93–94, <https://doi.org/10.1029/2008EO100001>, 2008.

828 Lipscomb, W. H., Price, S. F., Hoffman, M. J., Leguy, G. R., Bennett, A. R., Bradley, S. L., Evans, K. J., Fyke, J. G.,
829 Kennedy, J. H., Perego, M., Ranken, D. M., Sacks, W. J., Salinger, A. G., Vargo, L. J., and Worley, P. H.: Description and
830 evaluation of the Community Ice Sheet Model (CISM) v2.1, *Geoscientific Model Development*, 12, 387–424,
831 <https://doi.org/10.5194/gmd-12-387-2019>, 2019.

832 Lliboutry, L. A. and Duval, P.: Various isotropic and anisotropic ices found in glaciers and polar ice caps and their
833 corresponding rheologies, *Annals of Geophysics*, 3, 207–224, 1985.

834 Lowry, D. P., Gollledge, N. R., Bertler, N. A. N., Jones, R. S., McKay, R., and Stutz, J.: Geologic controls on ice sheet
835 sensitivity to deglacial climate forcing in the Ross Embayment, Antarctica, *Quaternary Science Advances*, 1, 100002,
836 <https://doi.org/10.1016/j.qsa.2020.100002>, 2020.

- 837 Maier, N., Gimbert, F., and Gillet-Chaulet, F.: Threshold response to melt drives large-scale bed weakening in Greenland,
838 *Nature*, 607, 714–720, <https://doi.org/10.1038/s41586-022-04927-3>, 2022.
- 839 Mair, D., Nienow, P., Sharp, M., Wohlleben, T., and Willis, I.: Influence of subglacial drainage system evolution on glacier
840 surface motion: Haut Glacier d’Arolla, Switzerland, *Journal of Geophysical Research: Solid Earth*, 107, EPM 8-1-EPM 8-13,
841 <https://doi.org/10.1029/2001JB000514>, 2002.
- 842 Mangeney, A. and Califano, F.: The shallow ice approximation for anisotropic ice: Formulation and limits, *Journal of*
843 *Geophysical Research: Solid Earth*, 103, 691–705, <https://doi.org/10.1029/97JB02539>, 1998.
- 844 Martin, J., Davies, B. J., Jones, R., and Thorndycraft, V.: Modelled sensitivity of Monte San Lorenzo ice cap, Patagonian
845 Andes, to past and present climate, *Frontiers in Earth Science*, 10, <https://doi.org/10.3389/feart.2022.831631>, 2022.
- 846 Marzeion, B., Hock, R., Anderson, B., Bliss, A., Champollion, N., Fujita, K., Huss, M., Immerzeel, W. W., Kraaijenbrink,
847 P., Malles, J.-H., Maussion, F., Radić, V., Rounce, D. R., Sakai, A., Shannon, S., van de Wal, R., and Zekollari, H.:
848 Partitioning the Uncertainty of Ensemble Projections of Global Glacier Mass Change, *Earth’s Future*, 8, e2019EF001470,
849 <https://doi.org/10.1029/2019EF001470>, 2020.
- 850 Masiokas, M. H., Christie, D. A., Le Quesne, C., Pitte, P., Ruiz, L., Villalba, R., Luckman, B. H., Berthier, E., Nussbaumer,
851 S. U., González-Reyes, A., McPhee, J., and Barcaza, G.: Reconstructing the annual mass balance of the Echaurren Norte
852 glacier (Central Andes, 33.5° S) using local and regional hydroclimatic data, *The Cryosphere*, 10, 927–940,
853 <https://doi.org/10.5194/tc-10-927-2016>, 2016.
- 854 Masiokas, M. H., Rabatel, A., Rivera, A., Ruiz, L., Pitte, P., Ceballos, J. L., Barcaza, G., Soruco, A., Bown, F., Berthier, E.,
855 Dussaillant, I., and MacDonell, S.: A Review of the Current State and Recent Changes of the Andean Cryosphere, *Frontiers*
856 *in Earth Science*, 8, <https://doi.org/10.3389/feart.2020.00099>, 2020.
- 857 Maussion, F., Butenko, A., Champollion, N., Dusch, M., Eis, J., Fourteau, K., Gregor, P., Jarosch, A. H., Landmann, J.,
858 Oesterle, F., Recinos, B., Rothenpieler, T., Vlug, A., Wild, C. T., and Marzeion, B.: The Open Global Glacier Model
859 (OGGM) v1.1, *Geoscientific Model Development*, 12, 909–931, <https://doi.org/10.5194/gmd-12-909-2019>, 2019.
- 860 Millan, R., Mouginot, J., Rabatel, A., and Morlighem, M.: Ice velocity and thickness of the world’s glaciers, *Nature*
861 *Geoscience*, 15, 124–129, <https://doi.org/10.1038/s41561-021-00885-z>, 2022.
- 862 Moreno-Parada, D., Alvarez-Solas, J., Blasco, J., Montoya, M., and Robinson, A.: Simulating the Laurentide Ice Sheet of the
863 Last Glacial Maximum, *The Cryosphere*, 17, 2139–2156, <https://doi.org/10.5194/tc-17-2139-2023>, 2023.
- 864 Nienow, P. W., Hubbard, A. L., Hubbard, B. P., Chandler, D. M., Mair, D. W. F., Sharp, M. J., and Willis, I. C.:
865 Hydrological controls on diurnal ice flow variability in valley glaciers, *Journal of Geophysical Research: Earth Surface*, 110,
866 <https://doi.org/10.1029/2003JF000112>, 2005.
- 867 Núñez Mejía, S., Villegas-Lituma, C., Crespo, P., Córdova, M., Gualán, R., Ochoa, J., Guzmán, P., Ballari, D., Chávez, A.,
868 Mendoza Paz, S., Willems, P., and Ochoa-Sánchez, A.: Downscaling precipitation and temperature in the Andes: applied
869 methods and performance—a systematic review protocol, *Environmental Evidence*, 12, 29, [https://doi.org/10.1186/s13750-](https://doi.org/10.1186/s13750-023-00323-0)
870 [023-00323-0](https://doi.org/10.1186/s13750-023-00323-0), 2023.
- 871 Payne, A. J., Nowicki, S., Abe-Ouchi, A., Agosta, C., Alexander, P., Albrecht, T., Asay-Davis, X., Aschwanden, A., Barthel,
872 A., Bracegirdle, T. J., Calov, R., Chambers, C., Choi, Y., Cullather, R., Cuzzone, J., Dumas, C., Edwards, T. L., Felikson,
873 D., Fettweis, X., Galton-Fenzi, B. K., Goelzer, H., Gladstone, R., Golledge, N. R., Gregory, J. M., Greve, R., Hattermann,
874 T., Hoffman, M. J., Humbert, A., Huybrechts, P., Jourdain, N. C., Kleiner, T., Munneke, P. K., Larour, E., Le clec’h, S., Lee,

875 V., Leguy, G., Lipscomb, W. H., Little, C. M., Lowry, D. P., Morlighem, M., Nias, I., Pattyn, F., Pelle, T., Price, S. F.,
876 Quiquet, A., Reese, R., Rückamp, M., Schlegel, N.-J., Seroussi, H., Shepherd, A., Simon, E., Slater, D., Smith, R. S.,
877 Straneo, F., Sun, S., Tarasov, L., Trusel, L. D., Van Breedam, J., van de Wal, R., van den Broeke, M., Winkelmann, R.,
878 Zhao, C., Zhang, T., and Zwinger, T.: Future Sea Level Change Under Coupled Model Intercomparison Project Phase 5 and
879 Phase 6 Scenarios From the Greenland and Antarctic Ice Sheets, *Geophysical Research Letters*, 48, e2020GL091741,
880 <https://doi.org/10.1029/2020GL091741>, 2021.

881 Pepin, N., Bradley, R. S., Diaz, H. F., Baraer, M., Caceres, E. B., Forsythe, N., Fowler, H., Greenwood, G., Hashmi, M. Z.,
882 Liu, X. D., Miller, J. R., Ning, L., Ohmura, A., Palazzi, E., Rangwala, I., Schöner, W., Severskiy, I., Shahgedanova, M.,
883 Wang, M. B., Williamson, S. N., Yang, D. Q., and Mountain Research Initiative, E. D. W. W. G.: Elevation-dependent
884 warming in mountain regions of the world, *Nature Climate Change*, 5, 424–430, <https://doi.org/10.1038/nclimate2563>, 2015.

885 Phipps, S. J., Roberts, J. L., and King, M. A.: An iterative process for efficient optimisation of parameters in geoscientific
886 models: a demonstration using the Parallel Ice Sheet Model (PISM) version 0.7.3, *Geosci. Model Dev.*, 14, 5107–5124,
887 <https://doi.org/10.5194/gmd-14-5107-2021>, 2021.

888 Pittard, M. L., Whitehouse, P. L., Bentley, M. J., and Small, D.: An ensemble of Antarctic deglacial simulations constrained
889 by geological observations, *Quaternary Science Reviews*, 298, 107800, <https://doi.org/10.1016/j.quascirev.2022.107800>,
890 2022.

891 Potter, E. R., Fyffe, C. L., Orr, A., Quincey, D. J., Ross, A. N., Rangescroft, S., Medina, K., Burns, H., Llacza, A., Jacome,
892 G., Hellström, R. Å., Castro, J., Cochachin, A., Montoya, N., Loarte, E., and Pellicciotti, F.: A future of extreme
893 precipitation and droughts in the Peruvian Andes, *npj Climate and Atmospheric Science*, 6, 96,
894 <https://doi.org/10.1038/s41612-023-00409-z>, 2023.

895 Rabatel, A., Francou, B., Soruco, A., Gomez, J., Cáceres, B., Ceballos, J. L., Basantes, R., Vuille, M., Sicart, J. E., Huggel,
896 C., Scheel, M., Lejeune, Y., Arnaud, Y., Collet, M., Condom, T., Consoli, G., Favier, V., Jomelli, V., Galarraga, R., Ginot,
897 P., Maisincho, L., Mendoza, J., Ménégou, M., Ramirez, E., Ribstein, P., Suarez, W., Villacis, M., and Wagnon, P.: Current
898 state of glaciers in the tropical Andes: a multi-century perspective on glacier evolution and climate change, *The Cryosphere*,
899 7, 81–102, <https://doi.org/10.5194/tc-7-81-2013>, 2013.

900 Richardson, A., Carr, R., and Cook, S.: Investigating the Past, Present and Future Responses of Shallap and Zongo Glaciers,
901 Tropical Andes, to the El Niño Southern Oscillation, *Journal of Glaciology*, 1–50, <https://doi.org/10.1017/jog.2023.107>,
902 2024.

903 Roe, G. H. and Baker, M. B.: Glacier response to climate perturbations: an accurate linear geometric model, *Journal of*
904 *Glaciology*, 60, 670–684, <https://doi.org/10.3189/2014JoG14J016>, 2014.

905 Rougier, J.: Setting up your simulator, 2015.

906 Rounce, D. R., Khurana, T., Short, M. B., Hock, R., Shean, D. E., and Brinkerhoff, D. J.: Quantifying parameter uncertainty
907 in a large-scale glacier evolution model using Bayesian inference: application to High Mountain Asia, *Journal of Glaciology*,
908 66, 175–187, <https://doi.org/10.1017/jog.2019.91>, 2020.

909 Rounce, D. R., Hock, R., Maussion, F., Hugonnet, R., Kochtitzky, W., Huss, M., Berthier, E., Brinkerhoff, D., Compagno,
910 L., Copland, L., Farinotti, D., Menounos, B., and McNabb, R. W.: Global glacier change in the 21st century: Every increase
911 in temperature matters, *Science*, 379, 78–83, <https://doi.org/doi:10.1126/science.abo1324>, 2023.

912 Schmidt, L. S., Adalgeirsdóttir, G., Pálsson, F., Langen, P. L., Gudmundsson, S., and Björnsson, H.: Dynamic simulations of
913 Vatnajökull ice cap from 1980 to 2300, *Journal of Glaciology*, 66, 97–112, <https://doi.org/10.1017/jog.2019.90>, 2020.

- 914 Schoof, C.: A variational approach to ice stream flow, *Journal of Fluid Mechanics*, 556, 227–251,
915 <https://doi.org/10.1017/S0022112006009591>, 2006.
- 916 Seguinot, J., Khroulev, C., Rogozhina, I., Stroeven, A. P., and Zhang, Q.: The effect of climate forcing on numerical
917 simulations of the Cordilleran ice sheet at the Last Glacial Maximum, *The Cryosphere*, 8, 1087–1103,
918 <https://doi.org/10.5194/tc-8-1087-2014>, 2014.
- 919 [Seguinot, J.: Spatial and seasonal effects of temperature variability in a positive degree-day glacier surface mass-balance
920 model. *Journal of Glaciology*, 59, 1202–1204. <https://doi.org/10.3189/2013JoG13J081>, 2017.](#)
- 921 Seguinot, J., Ivy-Ochs, S., Jouvet, G., Huss, M., Funk, M., and Preusser, F.: Modelling last glacial cycle ice dynamics in the
922 Alps, *The Cryosphere*, 12, 3265–3285, <https://doi.org/10.5194/tc-12-3265-2018>, 2018.
- 923 Seroussi, H., Pelle, T., Lipscomb, W. H., Abe-Ouchi, A., Albrecht, T., Alvarez-Solas, J., Asay-Davis, X., Barre, J.-B.,
924 Berends, C. J., Bernaldes, J., Blasco, J., Caillet, J., Chandler, D. M., Coulon, V., Cullather, R., Dumas, C., Galton-Fenzi, B.
925 K., Garbe, J., Gillet-Chaulet, F., Gladstone, R., Goelzer, H., Gолledge, N., Greve, R., Gudmundsson, G. H., Han, H. K.,
926 Hillebrand, T. R., Hoffman, M. J., Huybrechts, P., Jourdain, N. C., Klose, A. K., Langebroek, P. M., Leguy, G. R., Lowry,
927 D. P., Mathiot, P., Montoya, M., Morlighem, M., Nowicki, S., Pattyn, F., Payne, A. J., Quiquet, A., Reese, R., Robinson, A.,
928 Saraste, L., Simon, E. G., Sun, S., Twarog, J. P., Trusel, L. D., Urruty, B., Van Breedam, J., van de Wal, R. S. W., Wang, Y.,
929 Zhao, C., and Zwinger, T.: Evolution of the Antarctic Ice Sheet Over the Next Three Centuries From an ISMIP6 Model
930 Ensemble, *Earth's Future*, 12, e2024EF004561, <https://doi.org/10.1029/2024EF004561>, 2024.
- 931 Tadono, T., Ishida, H., Oda, F., Naito, S., Minakawa, K., and Iwamoto, H.: Precise Global DEM Generation by ALOS
932 PRISM, *ISPRS Annals of the Photogrammetry, Remote Sensing and Spatial Information Sciences*, II-4, 71–76,
933 <https://doi.org/10.5194/isprsannals-II-4-71-2014>, 2014.
- 934 Talchabhadel, R., Nakagawa, H., Kawaike, K., Yamanoi, K., and Thapa, B. R.: Assessment of vertical accuracy of open
935 source 30m resolution space-borne digital elevation models, *Geomatics, Natural Hazards and Risk*, 12, 939–960,
936 <https://doi.org/10.1080/19475705.2021.1910575>, 2021.
- 937 Taylor, L. S., Quincey, D. J., Smith, M. W., Potter, E. R., Castro, J., and Fyffe, C. L.: Multi-Decadal Glacier Area and Mass
938 Balance Change in the Southern Peruvian Andes, *Frontiers in Earth Science*, 10, <https://doi.org/10.3389/feart.2022.863933>,
939 2022.
- 940 [Treverrow, A., Budd, W. F., Jacka, T. H., and Warner, R. C.: The tertiary creep of polycrystalline ice: experimental evidence
941 for stress-dependent levels of strain-rate enhancement, *Journal of Glaciology*, 58, 301–314. \[https://doi.org/
942 10.3189/2012JoG11J149\]\(https://doi.org/10.3189/2012JoG11J149\), 2012.](#)
- 943 Tulaczyk, S., Kamb, W. B., and Engelhardt, H. F.: Basal mechanics of Ice Stream B, west Antarctica: 1. Till mechanics,
944 *Journal of Geophysical Research: Solid Earth*, 105, 463–481, <https://doi.org/10.1029/1999JB900329>, 2000.
- 945 Verjans, V. and Robel, A.: Accelerating Subglacial Hydrology for Ice Sheet Models With Deep Learning Methods,
946 *Geophysical Research Letters*, 51, e2023GL105281, <https://doi.org/10.1029/2023GL105281>, 2024.
- 947 Vuille, M., Francou, B., Wagnon, P., Juen, I., Kaser, G., Mark, B. G., and Bradley, R. S.: Climate change and tropical
948 Andean glaciers: Past, present and future, *Earth-Science Reviews*, 89, 79–96,
949 <https://doi.org/10.1016/j.earscirev.2008.04.002>, 2008.
- 950 Weertman, J.: On the Sliding of Glaciers, *Journal of Glaciology*, 3, 33–38, <https://doi.org/10.3189/S0022143000024709>,
951 1957.

952 Weis, M., Greve, R., and Hutter, K.: Theory of shallow ice shelves, *Continuum Mechanics and Thermodynamics*, 11, 15–50,
953 <https://doi.org/10.1007/s001610050102>, 1999.

954 Wilson, R., Glasser, N. F., Reynolds, J. M., Harrison, S., Anaconda, P. I., Schaefer, M., and Shannon, S.: Glacial lakes of the
955 Central and Patagonian Andes, *Global and Planetary Change*, 162, 275–291,
956 <https://doi.org/10.1016/j.gloplacha.2018.01.004>, 2018.

957 Winkelmann, R., Martin, M. A., Haseloff, M., Albrecht, T., Bueler, E., Khroulev, C., and Levermann, A.: The Potsdam
958 Parallel Ice Sheet Model (PISM-PIK) – Part 1: Model description, *The Cryosphere*, 5, 715–726, <https://doi.org/10.5194/tc-5-715-2011>, 2011.

960 Wolff, I. W., Glasser, N. F., Harrison, S., Wood, J. L., and Hubbard, A.: A steady-state model reconstruction of the
961 patagonian ice sheet during the last glacial maximum, *Quaternary Science Advances*, 12, 100103,
962 <https://doi.org/10.1016/j.qsa.2023.100103>, 2023.

963 Yan, Q., Wei, T., and Zhang, Z.: Modeling the climate sensitivity of Patagonian glaciers and their responses to climatic
964 change during the global last glacial maximum, *Quaternary Science Reviews*, 288, 107582,
965 <https://doi.org/10.1016/j.quascirev.2022.107582>, 2022.

966 Yan, Q., Wei, T., and Zhang, Z.: Modeling the timing and extent of glaciations over southeastern Tibet during the last glacial
967 stage, *Palaeogeography, Palaeoclimatology, Palaeoecology*, 610, 111336, <https://doi.org/10.1016/j.palaeo.2022.111336>,
968 2023.

969 Žebre, M., Sarikaya, M. A., Stepišnik, U., Colucci, R. R., Yıldırım, C., Çiner, A., Candaş, A., Vlahović, I., Tomljenović, B.,
970 Matoš, B., and Wilcken, K. M.: An early glacial maximum during the last glacial cycle on the northern Velebit Mt. (Croatia),
971 *Geomorphology*, 392, 107918, <https://doi.org/10.1016/j.geomorph.2021.107918>, 2021.

972 [Zeitiz, M., Reese, R., Beckmann, J., Krebs-Kanzow, U., and Winkelmann, R.: Impact of the melt–albedo feedback on the
973 future evolution of the Greenland Ice Sheet with PISM-dEBM-simple. *The Cryosphere*, 15, 5739–5764,
974 <https://doi.org/10.5194/tc-15-5739-2021>, 2021.](https://doi.org/10.5194/tc-15-5739-2021)

975 Zekollari, H., Schuster, L., Maussion, F., Hock, R., Marzeion, B., Rounce, D. R., Compagno, L., Fujita, K., Huss, M., James,
976 M., Kraaijenbrink, P. D. A., Lipscomb, W. H., Minallah, S., Oberrauch, M., Van Tricht, L., Champollion, N., Edwards, T.,
977 Farinotti, D., Immerzeel, W., Leguy, G., and Sakai, A.: Glacier preservation doubled by limiting warming to 1.5°C versus
978 2.7°C, *Science*, 388, 979–983, <https://doi.org/10.1126/science.adu4675>, 2025.

979 Zinck, A. S. P. and Grinsted, A.: Brief communication: Estimating the ice thickness of the Müller Ice Cap to support
980 selection of a drill site, *The Cryosphere*, 16, 1399–1407, <https://doi.org/10.5194/tc-16-1399-2022>, 2022.

981 Zoet, L. K. and Iverson, N. R.: A slip law for glaciers on deformable beds, *Science*, 368, 76–78,
982 <https://doi.org/10.1126/science.aaz1183>, 2020.

983